University of Reading

Preparation of mucoadhesive methacrylated chitosan nanoparticles for delivery of ciprofloxacin

Article

Accepted Version

Jalal, R. R., Ways, T. M. M., Elella, M. H. A., Hassan, D. A. and Khutoryanskiy, V. V. ORCID: https://orcid.org/0000-0002-7221-2630 (2023) Preparation of mucoadhesive methacrylated chitosan nanoparticles for delivery of ciprofloxacin. International Journal of Biological Macromolecules, 242 (Part4). 124980. ISSN 0141-8130 doi: 10.1016/j.ijbiomac.2023.124980 Available at https://centaur.reading.ac.uk/112237/

It is advisable to refer to the publisher's version if you intend to cite from the work. See Guidance on citing.

To link to this article DOI: http://dx.doi.org/10.1016/j.ijbiomac.2023.124980

Publisher: Elsevier

All outputs in CentAUR are protected by Intellectual Property Rights law, including copyright law. Copyright and IPR is retained by the creators or other copyright holders. Terms and conditions for use of this material are defined in the End User Agreement.

University of Reading

www.reading.ac.uk/centaur

CentAUR

Central Archive at the University of Reading

Reading's research outputs online

Research Paper

Preparation of Mucoadhesive Methacrylated Chitosan Nanoparticles for Delivery of Ciprofloxacin

Renas Rzgar Jalal[a], Twana Mohammed M. Ways[a,*], Mahmoud H. Abu Elella[b,c], Diyar Ahmed Hassan[d], Vitaliy V. Khutoryanskiy[b]

[a.] Department of Pharmaceutics, College of Pharmacy, University of Sulaimani, Sulaimani, 46001, Kurdistan Region, Iraq.
[b.] Reading School of Pharmacy, University of Reading, Whiteknights, Reading, RG6 6AD, United Kingdom.
[c.] Chemistry Department, Faculty of Science, Cairo University, Giza, 12613, Egypt.
[d.] Pioneer Co. for Pharmaceutical Industries, Sulaimani, 46001, Kurdistan Region, Iraq.
[*]Correspondence: twana.mohammed@univsul.edu.iq

Abstract

Mucoadhesive polymers and their nanoparticles have attracted a lot of attention in pharmaceutical applications, especially transmucosal drug delivery (TDD). Mucoadhesive polysaccharide-based nanoparticles, particularly chitosan, and its derivatives, are widely used for TDD owing to their outstanding features such as biocompatibility, mucoadhesive, and absorption-enhancing properties. Herein, this study aimed to design potential mucoadhesive nanoparticles for the delivery of ciprofloxacin based on methacrylated chitosan (MeCHI) using the ionic gelation method in the presence of sodium tripolyphosphate (TPP) and compared them with the unmodified chitosan nanoparticles. In this study, different experimental conditions including the polymer to TPP mass ratios, NaCl, and TPP concentration were changed to achieve unmodified and MeCHI nanoparticles with the smallest particle size and lowest polydispersity index. At 4:1 polymer /TPP mass ratio, both chitosan and MeCHI nanoparticles had the smallest size (133±5 nm and 206±9 nm, respectively). MeCHI nanoparticles were generally larger and slightly more polydisperse than the unmodified chitosan nanoparticles. Ciprofloxacin-loaded MeCHI nanoparticles had the highest encapsulation efficiency (69±13%) at 4:1 MeCHI /TPP mass ratio and 0.5 mg/mL TPP, but similar encapsulation efficiency to that of their chitosan counterpart at 1 mg/mL TPP. They also provided a more sustained and slower drug release compared to their chitosan counterpart. Additionally, the

mucoadhesion (retention) study on sheep abomasum mucosa showed that ciprofloxacin-loaded MeCHI nanoparticles with optimized TPP concentration had better retention than the unmodified chitosan counterpart. The percentage of the remained ciprofloxacin-loaded MeCHI and chitosan nanoparticles on the mucosal surface was 96% and 88%, respectively. Therefore, MeCHI nanoparticles have an excellent potential for applications in drug delivery.

Keywords: Chitosan; Methacrylated chitosan; Mucoadhesion; Nanoparticles; Ciprofloxacin; Drug delivery

1. Introduction

Mucoadhesive drug delivery systems are the drug carriers which have the ability to adhere to the mucus layer covering the mucosal membranes. The mucoadhesion of the drug delivery systems increases the residence time of the drug at the site of application and/or absorption and may enhance the absorption of the drug through mucosal membranes [1-3]. Increasing the residence time of the drug achieved by mucoadhesive drug delivery systems can significantly decrease the frequency of drug administration and therefore improve the patients' compliance. These systems can also be used for targeting a drug to a specific region of the body for extended periods of time, resulting in decreased systemic drug exposure and minimizing the side effects of the drugs [2,4].

Mucoadhesive drug delivery systems include different formulations such as tablets [5], patches [6], suppositories [7,8], gels [9], liposomes [10,11], microparticles [12], and nanoparticles [13-16]. Among these, the mucoadhesive nanoparticles have attracted the attention of researchers owing to their small size, better distribution throughout the mucosal tissues, better physical stability [17,18], high drug loading [19], and feasibility for applications via different routes of administration, including oral [20,21], rectal [22], vaginal [23], nasal [24], ocular [25], and inhalational [26,27].

Mucoadhesive nanoparticles are normally prepared using hydrophilic polymers as excipients in their formulations. A typical example of these polymers is chitosan which is a cationic polysaccharide with unique properties including hydrophilicity, safety, biodegradability, drug permeation-enhancing ability, and mucoadhesivity [28,29]. The main mechanism involved in the mucoadhesion of chitosan is the electrostatic attraction between chitosan and the mucin glycoproteins of mucus on mucosal surfaces [30-32]. Under physiological conditions, the

positively charged amino groups of chitosan bind to the negatively charged sialic acid and sulfonic acid groups of mucin [33-35]. This electrostatic attraction is generally considered to be a weak interaction that only provides a limited mucoadhesive force being in many cases inadequate to guarantee the prolonged retention of drug delivery systems on mucosal surfaces [36]. Therefore, different chitosan derivatives including thiolated [37], boronated [38], acrylated [39], and methacrylated chitosan [36] have been developed that can adhere to mucosal surfaces via covalent bonds significantly stronger than the unmodified chitosan. The mucoadhesive properties of thiolated chitosan in many different formulations have been extensively studied by Bernkop-Schnürch group [37]. Khutoryanskiy et al. [36] previously demonstrated that methacryloylation of chitosan to form MeCHI dramatically improved its mucoadhesive properties due to the possibility of forming covalent bonds between methacryloyl groups of MeCHI and thiol groups present in mucin glycoproteins. They evaluated the mucoadhesive properties for solutions of MeCHI on porcine bladder mucosa. However, it was not clear that the enhanced mucoadhesivity of MeCHI can also be achieved if this polymer is formulated as nanoparticles.

Many studies have also reported the formation of chitosan polyelectrolyte complexes through interactions between two oppositely charged polymers for example chitosan and natural anionic polymers including alginate, pectin, carrageenan, xanthan gum, hyaluronic acid and fucoidan for the development of mucoadhesive nanoparticles for oral drug delivery [40-43]. The formation of polyelectrolyte complexes limits the disadvantages of individual polymers, such as limited mucoadhesivity, poor mechanical durability and instability in vivo, and poor aqueous solubility at physiological pH (ranging from 1.2 to 8) while retaining the biological activities of the active ingredient, leading to the formation of new materials with better mucoadhesive and permeation-enhancement properties as well as good stability at physiological pH [41,44]. However, the process of formation of polyelectrolyte complexes depends on more factors, for example, the properties of the anionic polymer such as its molecular weight and viscosity [40].

The potential of using MeCHI for preparing nanoparticles was not explored previously. MeCHI nanoparticles are expected to have a better potential as drug nanocarriers compared to other types of nanoparticles as they are prepared using safe and biocompatible polymers [36]. Due to the availability of various functional groups and the swelling behavior of MeCHI nanoparticles, they could have a higher drug loading capacity than the non-functionalized inorganic nanoparticles.

Therefore, the aims of this study were to prepare chitosan and MeCHI nanoparticles and compare their physicochemical and mucoadhesive characteristics. To the best of our knowledge, this is the first study that reports the preparation of ciprofloxacin-loaded MeCHI nanoparticles and shows their enhanced mucoadhesive properties. The novelty of this study includes developing a method of preparation of a novel chitosan derivative (MeCHI)-based nanoparticles as well as establishing a new method for the evaluation of mucoadhesive properties of the prepared MeCHI nanoparticles. The feasibility of loading drugs into these novel nanoparticles was also explored using ciprofloxacin as a model drug.

Several studies have reported the preparation of mucoadhesive chitosan nanoparticles using the ionotropic gelation method in the presence of TPP and showed their potential as a vehicle for the delivery of drugs with various physicochemical properties [45]. However, recently, the preparation of chemically modified chitosan derivative nanoparticles has shown potential interest to improve the mucoadhesive property of chitosan for delivering therapeutic drugs to the target position in a short time. Therefore, our research group is interested in designing potential mucoadhesive drug nanocarriers based on chitosan. To the best of our knowledge, the preparation of MeCHI nanoparticles using this relatively simple approach has not been reported until now. In this study, we have shown that it is possible to prepare MeCHI nanoparticles from MeCHI using the ionic gelation method in the presence of TPP as an ionic cross-linker. Therefore, this study significantly contributes to the development of novel excipients used in the formulation of drug-loaded nanoparticles and explores the techniques used in the preparation and characterization of such nanoparticles.

2. Materials and Methods

2.1. Materials

Low molecular weight chitosan (Sigma-Aldrich UK, with a degree of deacetylation 85%), sodium tripolyphosphate (TPP, Sigma-Aldrich UK), sodium chloride, sodium hydroxide (Merck, Germany), acetic acid (Gainland, UK) and methacrylic anhydride (Sigma-Aldrich, Gillingham, UK) were used in this study. Cellulose dialysis membrane (molecular weight cut-off 12–14 kDa)

was purchased from Medicell International Ltd. Ciprofloxacin HCl was provided by Pioneer Co. for Pharmaceutical Industries, Kurdistan Region, Iraq.

2.2. Experimental Methods

2.2.1. Synthesis of MeCHI

MeCHI was prepared via the reaction of chitosan and methacrylic anhydride at 40 ^{o}C in the dark according to our previously published protocol [36]. In brief, 1 g of chitosan was dissolved in 1% acetic acid under continuous stirring at room temperature (20 ^{o}C) overnight. Then 2 mL of methacrylic anhydride was slowly added to the above chitosan solution under continuous stirring for 12 hours at 40 ^{o}C in the dark. After 12 hours, the resulting product (MeCHI) was purified using dialysis with cellulose membrane (MWCO 12-14 kDa) against 5 L of deionized water in the dark for 72 hours (9 water changes were carried out). Following the dialysis, the purified MeCHI was frozen and then lyophilized using the Heto Power Dry LL 3000 freeze-drier. The prepared MeCHI sample was collected and stored in the fridge (4^{o} C) for further use. The successful preparation of MeCHI was confirmed using FTIR and ^{1}H NMR spectroscopy.

2.2.2. Characterization of MeCHI

The chemical structure of the prepared MeCHI was elucidated using Fourier-transform infrared spectroscopy (FTIR) and proton nuclear magnetic resonance (^{1}H NMR) spectroscopy and compared with unmodified chitosan. The FTIR spectra of chitosan and MeCHI were collected from 4000 to 600 cm^{-1} using Nicolet iS5-iD5 ATR FT-IR spectrometer (Thermo Scientific, UK). A 400 MHz ULTRASHIELD PLUS™ B-ACS 60 spectrometer was used to record the ^{1}H NMR spectra using D_2O acidified with trifluoroacetic acid as a solvent.

2.3. Preparation of Nanoparticles

Chitosan and MeCHI nanoparticles were prepared using an ionic cross-linking method in the presence of TPP [46,47]. Chitosan or MeCHI (1 mg/mL) were dissolved in 1% v/v acetic acid with or without NaCl under continuous stirring for 24 hours at room temperature. The insoluble chitosan or MeCHI was removed using a syringe filter (0.45 µm), then the pH of the solution was adjusted to 5.3 using 5 M NaOH solution. TPP was dissolved in distilled water to prepare a 1

mg/mL solution. Nanoparticle suspensions were prepared by the dropwise addition of TPP solution to the chitosan or MeCHI solutions with stirring (380 rpm) at room temperature. The suspended nanoparticles were stirred for additional 30 minutes at room temperature. Various parameters were changed to optimize the formulations and the details of the optimization steps are shown in the following sections.

2.3.1. Chitosan/MeCHI to TPP mass ratio

The nanoparticles were prepared at selected chitosan or MeCHI to TPP mass ratios (1:2, 1:1, 2:1, 3:1, 4:1, and 5:1) by changing the volume of the TPP solution which was added to the chitosan or MeCHI solution.

2.3.2. Addition of NaCl

Two formulations of each of the chitosan and MeCHI nanoparticles were prepared using NaCl. Chitosan or MeCHI (1 mg/mL) was dissolved in 1% v/v acetic acid containing 0.5 mg/mL NaCl. The solutions were kept under continuous stirring for 24 hours at room temperature. Nanoparticles were prepared at 4:1 and 5:1 chitosan or MeCHI to TPP mass ratio.

2.3.3. TPP concentration

Four formulations of each of the chitosan and MeCHI nanoparticles were prepared at a constant TPP solution concentration (0.5 mg/mL). Chitosan or MeCHI (1 mg/mL) was dissolved in 1% v/v acetic acid with or without NaCl. The nanoparticles were prepared at 4:1 and 5:1 chitosan/MeCHI to TPP mass ratio.

Chitosan and MeCHI nanoparticles were formulated at different polymer to cross-linker ratios whereas the concentration of the polymers was kept constant (1 mg/mL). In addition, two formulations of each chitosan and MeCHI nanoparticles were prepared using NaCl. Four formulations of each polymeric nanoparticle were prepared by changing TPP concentration at the same polymer to TPP mass ratio. Depending on the size and polydispersity index (PDI) of the unloaded nanoparticles, four formulations were then selected and used to prepare ciprofloxacin-loaded chitosan and MeCHI nanoparticles. Ciprofloxacin-loaded chitosan nanoparticles were prepared using a polymer to TPP mass ratio of 4:1 with and without NaCl. For the formulation of ciprofloxacin-loaded MeCHI nanoparticles, the polymer to TPP mass ratio was 4:1 with two

different TPP concentrations (0.5 and 1 mg/mL). NaCl was not used in the formulation of ciprofloxacin-loaded MeCHI nanoparticles.

2.3.4. Preparation of ciprofloxacin-loaded chitosan and MeCHI nanoparticles

After the optimization process of the blank nanoparticles, four formulations with the smallest mean particle size and the lowest PDI were selected to prepare ciprofloxacin-loaded chitosan/MeCHI nanoparticles. Chitosan or MeCHI was dissolved in 1% v/v acetic acid with or without NaCl to prepare 1 mg/mL polymers' solutions. The solutions were stirred for 24 hours at room temperature using a magnetic stirrer. Ciprofloxacin HCl (0.5 mg/mL) was added to the polymer solutions 20 minutes prior to the nanoparticles preparation. The insoluble chitosan or MeCHI was removed using a syringe filter (0.45 µm), then the pH of the solutions was adjusted to 5.3 using 5 M NaOH solution. TPP was dissolved in distilled water to prepare a 1 mg/mL TPP solution. Ciprofloxacin-loaded nanoparticles were prepared by the dropwise addition of TPP solution to the chitosan or MeCHI solutions with continuous stirring. The suspended nanoparticles were stirred for additional 30 minutes at room temperature.

2.4. Nanoparticle Characterization

2.4.1. Dynamic light scattering (DLS)

SZ-100z Dynamic Light Scattering (Horiba Jobin Jyovin, Japan) was used to measure the size distribution and zeta potential of the nanoparticles. Distilled water was used as a dispersion medium to dilute the nanoparticles (1:100). For the particle size analysis, the scattering angle was kept at 90 °C with a holder temperature of 25 °C, a refractive index of 1.58, and a medium viscosity of 0.892 mPa·s. Measurements were performed in triplicates and samples were equilibrated for 60 seconds per run using 12 µL quartz cuvettes prior to each measurement. A disposable zeta potential cell with carbon-coated electrodes was used for the zeta potential measurement. Smoluchowski model (Fka=1.5) was used to convert the electrophoretic mobility data to the zeta-potential values.

2.4.2. Transmission electron microscopy (TEM)

The morphology of the chitosan and MeCHI nanoparticles was studied using TEM (Carl Zess_EM1OC, Germany) at an accelerating voltage of 100 kV. One drop of nanoparticles suspensions was placed onto a carbon-coated copper grid and left to dry for 1 minute at room

temperature. The formulations were stained with 2% w/v phosphotungstic acid solution. The stained formulations were left to dry in the air at room temperature and then used for TEM imaging. The particle size was measured using ImageJ-Java 8 software.

2.5. Encapsulation Efficiency (EE) and Loading Capacity (LC)

The drug-loaded nanoparticle suspensions were precipitated and separated from the free ciprofloxacin using a centrifugation method (Maanlab, HC 02R, Sweden, 15,000 rpm, 2 ºC, 40 min). The free amount of ciprofloxacin in the supernatant was analyzed using UV-visible spectrophotometry (PharmaSpec, UV-1700, Japan) at λ_{max} of 277 nm. The concentration of ciprofloxacin in the supernatant was measured by referring to a calibration curve (Figure S1). The experiment was performed in triplicate, the EE and LC were calculated using equations 1 and 2, respectively.

$$\text{EE \%} = \frac{\text{Total amount of ciprofloxacin} - \text{Free amount of ciprofloxacin in supernatant}}{\text{Total amount of ciprofloxacin}} \times 100 \quad (1)$$

$$\text{LC \%} = \frac{\text{Total amount of ciprofloxacin} - \text{Free amount of ciprofloxaicin in supernatant}}{\text{Total weight of nanoparticles}} \times 100 \quad (2)$$

2.6. Ciprofloxacin Release

In vitro drug release was studied using a dialysis method in simulated gastric fluid (contained 0.2% w/v NaCl aqueous solution, and the pH was adjusted to 1.2 using 1 M HCl), and simulated intestinal fluid (made of 0.2 M phosphate buffer aqueous solution, pH 6.8). The ciprofloxacin-loaded chitosan/MeCHI nanoparticles suspensions were centrifuged (Maanlab, HC 02R, Sweden, 15000 rpm, 2 ºC, 40 min) to prepare the drug-loaded nanoparticles precipitates, which were washed with distilled water once. A specific amount of the precipitated ciprofloxacin-loaded nanoparticles (equivalent to 5 mg ciprofloxacin) was redispersed in 5 mL phosphate buffer (0.2 M, pH 5). The dialysis membrane was soaked in distilled water for one hour and washed with distilled water. 5 mL of the redispersed nanoparticles was transferred to the dialysis membrane (MWCO 14 kDa, Membra-Cell, USA). The dialysis membrane was tied by a clump at both sides and the middle part of the dialysis membrane was immersed in 30 mL simulated intestinal fluid or stimulated gastric fluid at 37±1 ºC under continuous stirring at 100 rpm. At a specific time interval, 2 mL of the dialysis medium was collected and replaced with the same volume of the freshly prepared phosphate buffer. The amount of ciprofloxacin released into the dialysis medium was measured

using UV-visible spectrophotometry at λ_{max} of 277 nm. The calibration curve was constructed from the absorbance of standard solutions of ciprofloxacin HCl (Figure S1).

2.7. Mucoadhesion Test

The mucoadhesion of chitosan and MeCHI nanoparticles was evaluated using an *ex vivo* wash-off method with some modifications [48-50]. The sheep stomach was obtained from animal slaughter, washed with distilled water, and stored in a freezer (-20 ºC). Prior to experiments, the tissues were thawed and a 2.5 ×7.5 cm piece of sheep abomasum mucosa was excised and carefully washed with 2 mL simulated gastric fluid. The simulated gastric fluid consisted of 0.2% NaCl solution adjusted to pH 1.8±0.1 using 1 M HCl solution [48]. The dissected stomach tissue was placed on a microscope slide. Then, 0.5 mL ciprofloxacin-loaded chitosan or MeCHI nanoparticles suspensions (containing 0.5 mg of ciprofloxacin) were placed on the tissues, then left for 5 minutes. The microscope slide was fixed at 45º angle relative to the horizontal surface. Then, the tissue was exposed to simulated gastric fluid (warmed at 37 ºC) at a constant flow rate (1 mL/minute). Finally, the wash fluid samples were collected at pre-determined time intervals 1, 2, 3, 4, 5, 10, 15, and 20 minutes. The amount of ciprofloxacin washed with stimulated gastric fluid was analyzed using HPLC (Waters, Alliance e2695, Empower software). The HPLC system consisted of a Micro-vacuum degasser, a quaternary pump, an autosampler (Alliance), and a UV detector. Reverse phase chromatography was used with an XBridge® C18 5µ 4.6×25 mm HPLC column. The mobile phase was acetonitrile:0.025 M phosphoric acid (pH 3 adjusted with trimethylamine, 13:87 volume ratio). An isocratic mode with a 1.5 mL/min flow rate was used. The injection volume was 10 µL and the analysis was conducted at λ_{max} of 278 nm and 30±1 ºC. The amount of ciprofloxacin in the washed samples was found using a calibration curve (Figure S2) prepared from standard solutions of ciprofloxacin HCl in simulated gastric fluid. The experiments were performed in triplicates, and the percentage of retained ciprofloxacin was found using equation 3.

$$\text{Retained } \% = \frac{\text{total drug used} - \text{drug collected after wash off at predetermined time}}{\text{total drug used}} * 100 \quad (3)$$

2.8. Stability Studies

2.8.1. Storage stability study

The physical stability of the prepared ciprofloxacin-loaded chitosan and MeCHI nanoparticles was assessed visually, and using DLS (Sz-100z, Horiba Jobin Jyovin, Japan). The general appearance of the nanoparticles including any precipitation and color change was assessed after six months at two different temperatures (4 ºC and 25 ºC). The size and PDI of the nanoparticles stored in fridge (4 ºC) were also analyzed using DLS.

2.8.2. pH stability study

The pH stability of ciprofloxacin-loaded chitosan and MeCHI nanoparticles in stimulated gastric fluid (pH 1.2) and simulated intestinal fluid (pH 6.8) was analyzed. The size and PDI were measured using DLS (Sz-100z, Horiba Jobin Jyovin, Japan). The nanoparticles were diluted to 1:100 with simulated gastric or intestinal fluid.

2.9. Statistical Analysis

All experiments were performed in triplicates and the data are expressed as mean ± standard deviation which was calculated using Microsoft Excel software. Statistical analysis was performed using the two-way analysis of variance (ANOVA), and a (Fischer´s LSD) post-hoc test using (GraphPad Prism version 9) software. A p-value of < 0.05 was considered statistically significant.

3. Results and Discussion

3.1. Synthesis and Structural Characterization of MeCHI

MeCHI was prepared by reacting chitosan with methacrylic anhydride (Figure S3). The components of the reaction mixture, the visual appearance, and the degree of methacrylation are shown in Table S1. The reaction resulted in 66% of the product yield and MeCHI had an off-white appearance.

The chemical structure of the prepared MeCHI was confirmed using FTIR and ^{1}H NMR spectroscopy. Figure 1 shows the FTIR spectra of chitosan and MeCHI. The FTIR spectrum of chitosan illustrates different absorption bands at 3267 cm^{-1} related to N-H and O-H vibration stretching bonds and 2877 cm^{-1} referred to stretching of C-H bond, 1647 cm^{-1} and 1418 cm^{-1} referred to symmetric and asymmetric vibrations of C=O (amide I) groups. Moreover, absorption bands appeared at 1559 cm^{-1} corresponded to the bending of N-H groups, and at 1154 cm^{-1} and

892 cm^{-1} corresponded to bending vibrations of glycosidic (C-O-C) bonds in the repeating unit of chitosan. The bands at 1060 cm^{-1} and 1033 cm^{-1} indicated the stretching vibration of secondary and primary alcohol groups (C-OH) in chitosan chains, respectively.

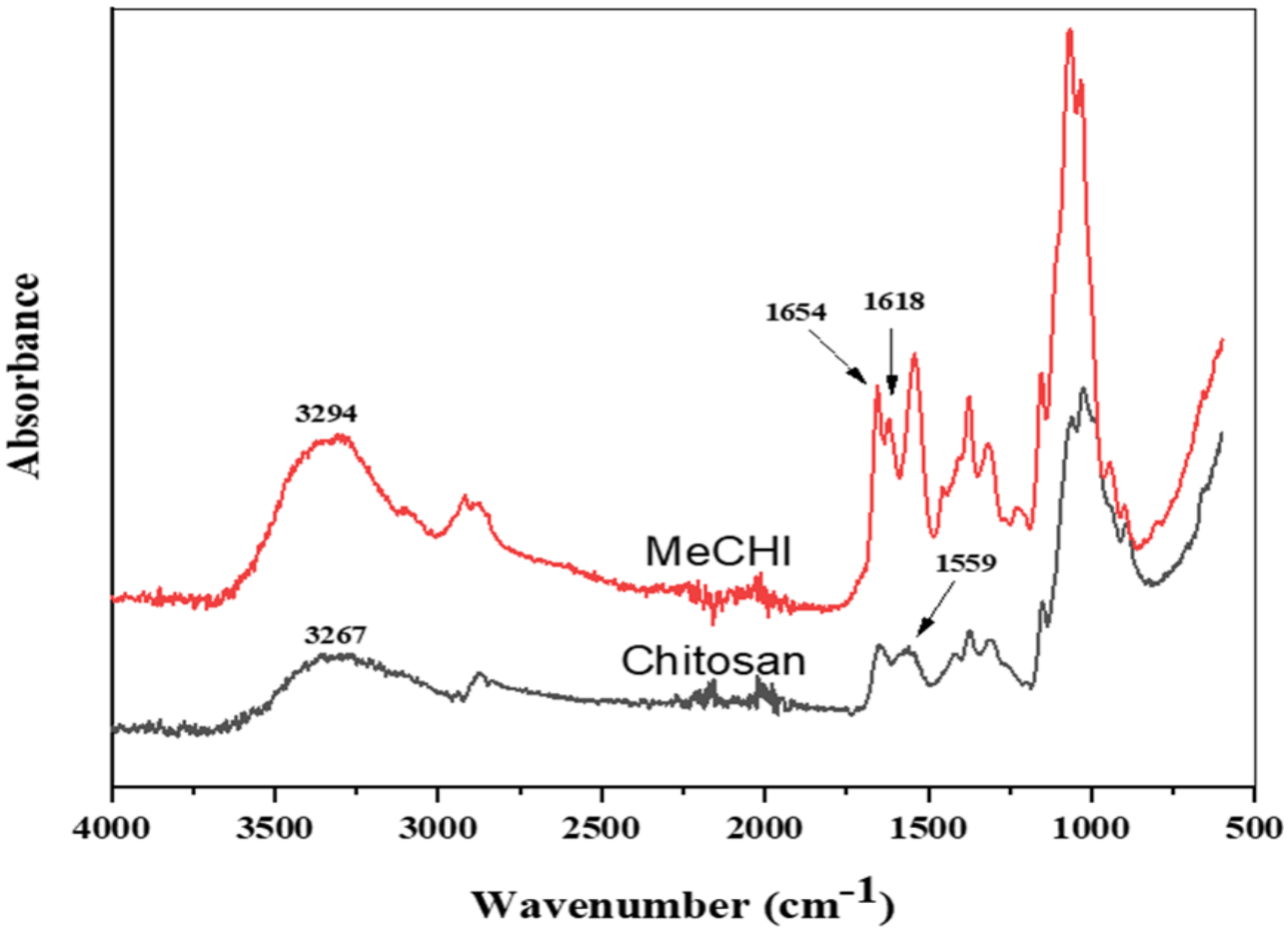

Figure 1. FTIR spectra of chitosan and MeCHI.

On the other hand, the FTIR spectrum of MeCHI shows the appearance of a new band at 1618 cm^{-1} due to the stretching of the alkenyl (C=C) group in the MeCHI structure. Additionally, the amide band at 1647 cm^{-1} in the chitosan spectrum shifted to the sharp absorption band at 1654 cm^{-1} referring to new amide (C=O) groups in the MeCHI structure.

Figure 2 shows the ^{1}H NMR spectra of both chitosan and MeCHI. The characteristic peaks of chitosan are observed at 2.0, 3.2, and 4.5 ppm related to *N*-acetylated methyl groups protons, protons attached to the second carbon atom, and anomeric proton (H1), respectively. Additionally,

multiplet peaks appeared at δ= 3.6 - 3.9 ppm, which are due to the protons attached to carbon atoms number 3-6 (30-33). On the other hand, the ^{1}H NMR spectrum of MeCHI illustrates the peaks of glucosamine ring's protons at 3.0-3.8 ppm, as well as the peaks of methyl protons of acetyl and methacrylamide groups of MeCHI at 1.65-1.90 ppm. Additionally, two singlet peaks at 5.3 and 5.6 ppm indicate the protons of methacrylated double bond (C=C) which conjugated with chitosan structure. Small peaks appeared at δ= 0.8-1.1 ppm, which are due to the protons of the inhibitor attaching to the methacrylic anhydride monomer. Moreover, a sharp peak at 4.7 ppm was observed which is related to the solvent (D_2O).

The degree of methacrylation of MeCHI was found using ^{1}H NMR spectra data according to equation (4). The ratio between the intensity of protons of methacrylate double bond groups from δ= 5.3 ppm to 5.6 ppm and the intensity of peaks of glucosamine ring's protons (δ= 3.0-3.8 ppm) was calculated. The degree of methacrylation of MeCHI was 28%.

$$\text{Methacrylation degree } \% = \frac{\text{Integral of methacrylate double bond protons}/2}{\text{Integral of glucosamine ring's protons (H2} - \text{H6)}/6} \times 100 \qquad (4)$$

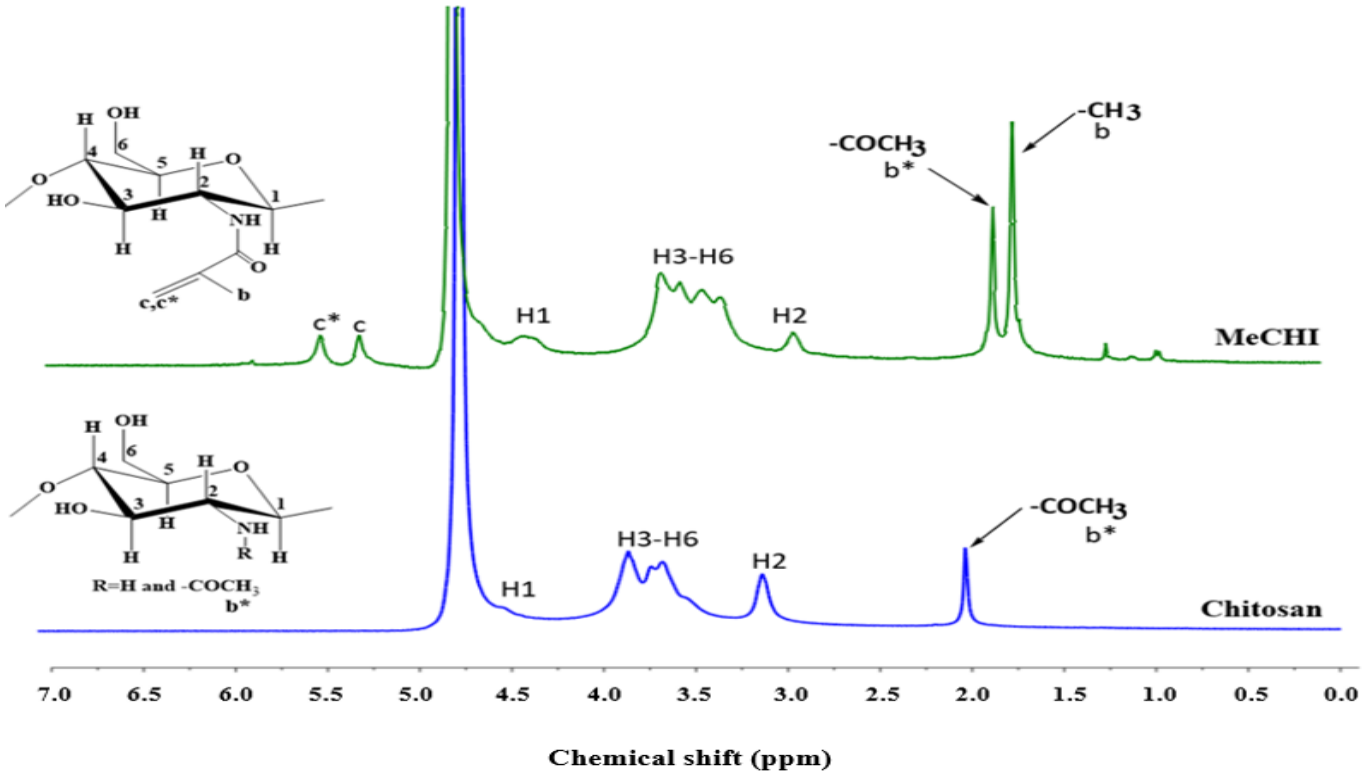

Figure 2. ^{1}H NMR spectra of chitosan and MeCHI

3.2. Characterization of Nanoparticles

Chitosan and MeCHI nanoparticles were prepared by ionic cross-linking of the positively charged chitosan or MeCHI and negatively charged anionic TPP. To prepare chitosan and MeCHI nanoparticles with different size, several possible experimental variables were used and the results were compared. Visual appearance, mean particle size, and PDI of both chitosan and MeCHI nanoparticles were evaluated.

Chitosan and MeCHI nanoparticles were formulated using different polymer to TPP ratios but the same polymer initial concentration (1 mg/mL). In addition, two formulations of both polymers were prepared in the presence of NaCl to explore the effects of ionic strength on the properties of the nanoparticles. Four formulations of each polymeric nanoparticle formulation were prepared by changing TPP concentration at the same polymer to TPP mass ratio.

The visual observation during the preparation of the nanoparticles revealed that the chitosan solutions changed from fully transparent to a translucent solution indicating the formation of the nanoparticles. However, this change in transparency was not observed with the MeCHI nanoparticles (Figure S4). The difference in the transparency of chitosan and MeCHI nanoparticle suspensions could be due to the difference in the optical properties, refractive index, size, and shape of the nanoparticles [51,52].

For chitosan, the transparency of nanoparticle suspensions changed with the change in the mass ratio of chitosan to TPP. As the mass of TPP increased, the turbidity of the solution increased, which reveals that the number of nanoparticles formed increases as the mass of TPP increases. This phenomenon indicates that as the TPP mass increases the number of negatively charged groups available to react with the positively charged groups of chitosan increases, leading to the formation of a larger number of nanoparticles [53]. This is in agreement with the study of Shafiei et. al. [54] who reported that the increase in the TPP mass increased the aggregation of chitosan nanoparticles.

At the polymer/TPP mass ratios of 1:2, 1:1, and 2:1, both chitosan and MeCHI nanoparticles underwent precipitation after 48 hours when stored at room temperature. The precipitation could be due to the decrease in the polymers to TPP mass ratio to less than the specific value (3:1) that is required to form nanoparticles. This could result in an increase in the number of nanoparticles

formed and subsequent aggregation of the nanoparticles due to the presence of the excessive amount of the negatively charged TPP available for binding with the positively charged groups of the already formed chitosan nanoparticles. This could be due to the fact that TPP can potentially form five ionic bonds with the amino groups of chitosan resulting in a single particle formation and subsequent aggregation of the individual particles [55]. In contrast, at polymer to TPP mass ratios of 3:1, 4:1, and 5:1, smaller nanoparticles were obtained which could be due to the decrease in the mass of TPP (the details of the data are available in the following sections). This is aligned with the study of Nunes et al. [56] who found that as the mass ratio of chitosan to TPP decreased from 3.5:1 to 1.75:1, the particle size of chitosan nanoparticles remained at the nano-range, but the further decrease in chitosan to TPP mass ratio to 0.85:1, the particle size increased to 1000 nm [56].

3.3. DLS Analysis

3.3.1. Polymer/TPP mass ratio

Mean particle size, Z-average size, and PDI of chitosan and MeCHI nanoparticles at 3:1, 4:1, and 5:1 polymer to TPP mass ratios were analyzed using DLS and the results are shown in Table 1. DLS analysis was not performed for formulations having polymer to TPP mass ratios of 1:2, 1:1, and 2:1 as they underwent precipitation immediately after their preparation. Mean particle size denotes for distribution of the size and a width for each separate size peak of the distribution The Z-average size is the intensity-weighted mean hydrodynamic size of the ensemble collection of particles measured by DLS. It is derived from a cumulants analysis of the measured correlation curve, wherein a single particle size is assumed and a single exponential fit is applied to the autocorrelation function [57]. The Z-average size could be smaller, equal to, or greater than the mean particle size depending on the width of the size distribution (homogeneity of the size) which is usually indicated by the PDI of the nanoparticles [57]. In this study, in addition to reporting the Z-average size values, the mean particle size was also used to compare the diameter of the prepared nanoparticles.

Table 1. Compositions and physicochemical properties of the unloaded chitosan and MeCHI nanoparticles (mean ± SD, n=3).

Polymer and salt in the nanoparticles	Chitosan to TPP mass ratio	TPP concentration (mg/mL)	Mean particle size (nm)	PDI	Z-average size (nm)	Zeta potential (mV)
Chitosan	3:1	1	135±9	0.212±0.032	129±4	2.36±1.12
Chitosan	4:1	1	133±5	0.402±0.145	120±4	12.50±0.26
Chitosan	5:1	1	146±8	0.259±0.137	142±7	6.26±2.58
Chitosan with NaCl	4:1	1	137±0.5	0.138±0.056	142±5	9.10±0.52
Chitosan with NaCl	5:1	1	173±20	0.265±0.148	142±1	2.46±1.76
Chitosan	4:1	0.5	191±7	0.192±0.138	180±7	18.93±1.40
Chitosan with NaCl	4:1	0.5	186±7	0.333±0.152	179±5	2.86±1.05
Chitosan	5:1	0.5	177±25	0.213±0.177	172±8	5.50±1.05
Chitosan with NaCl	5:1	0.5	177±14	0.296±0.195	167±23	8.96± 1.60
MeCHI	3:1	1	281±54	0.666±0.179	359±60	1.70±0.793
MeCHI	4:1	1	206±9	0.462±0.158	263±86	10.85±0.07
MeCHI	5:1	1	377±89	0.647±0.133	590±148	2.60±1.33
MeCHI with NaCl	4:1	1	334±18	0.513±0.228	368±34	10.33±1.59
MeCHI with NaCl	5:1	1	265±94	0.613±0.082	157±36	6.33±2.65
MeCHI	4:1	0.5	274±73	0.541±0.211	402±173	10.53±0.55
MeCHI with NaCl	4:1	0.5	566±210	0.762±0.131	244±12	1.66±0.85
MeCHI	5:1	0.5	521±100	0.664±0.241	254±11	1.20±0.81
MeCHI with NaCl	5:1	0.5	232±101	0.621±0.092	164±33	3.96±1.55

To better clarify the effects of polymer/TPP mass ratio on the properties of the nanoparticles, the mean particle size and PDI values of the chitosan and MeCHI nanoparticles at different chitosan/MeCHI to TPP mass ratios are shown in Figure 3. It is clear that there was no significant difference ($p > 0.05$) between the size of different chitosan nanoparticles prepared using different chitosan to TPP mass ratios. On the other hand, MeCHI nanoparticles, at the polymer/TPP mass ratio of 4:1, showed a significantly smaller particle size (206±9 nm) compared to the polymer/TPP mass ratios of 3:1, and 5:1 ($p < 0.05$, and $p < 0.001$, respectively). This is related to the necessity of the optimum polymer/crosslinker ratio to control the crosslinking of the polymer macromolecules and the compactness of the nanoparticles [58].

PDI is a measure of the dispersity (distribution width) in the size of nanoparticles. As the value of PDI decreases the monodispersity increases and indicates homogeneous size distribution. In contrast, a high PDI value indicates the nanoparticles are heterogeneously distributed and have a broad size distribution. The PDI values range from 0 to 1 and, generally, values smaller than 0.05 are rarely seen other than with highly monodisperse standards. On the other hand, values greater than 0.7 indicate that the sample has a broad size distribution [59]. Figure 3b shows the values of PDI of both chitosan and MeCHI nanoparticles. Changing the polymer/TPP mass ratio did not have any significant effect ($p > 0.05$) on the PDI of the nanoparticles.

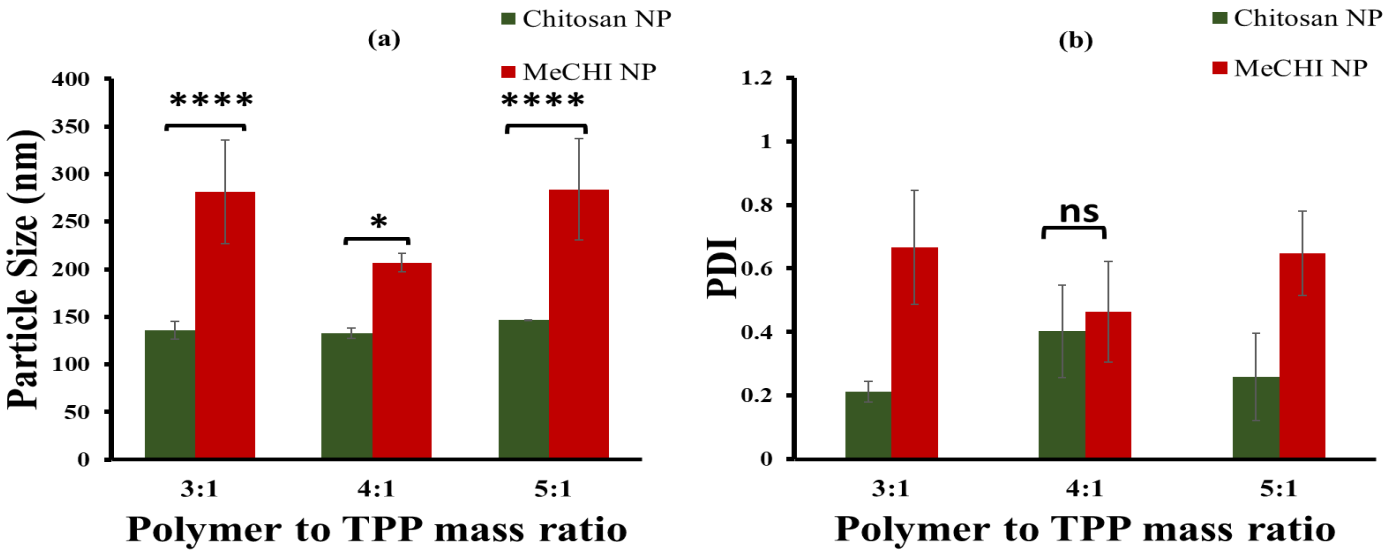

Figure 3. Effect of polymer to TPP mass ratio and type of polymer on mean particle size (a), and PDI (b) of chitosan and MeCHI nanoparticles at 1 mg/mL TPP and without NaCl. There is no significant difference ($p>0.05$) between the sizes and PDI values of chitosan nanoparticles at different polymer to TPP mass ratios. MeCHI nanoparticles have a smaller ($p<0.05$) size at a polymer to TPP mass ratio of 4:1 compared to other mass ratios, but they showed no significant difference in their PDI when prepared using different polymer to TPP mass ratios. (****) $p<0.0001$, (*): $p<0.05$, (ns): not significant, (NP): nanoparticles.

3.3.2. Effect of type of polymer

Chemical modification of chitosan can significantly improve the properties of chitosan including its antibacterial activities, antioxidant, mucoadhesive and permeation enhancing effects [28,60-62]. Additionally, changing the type of the polymer had a significant effect on the size of nanoparticles (Table 1 and Figure 3) The larger size of the MeCHI nanoparticles could be due to the less dense structure of the nanoparticles formed from MeCHI compared to chitosan. The particle size of MeCHI nanoparticles was significantly greater than the size of chitosan nanoparticles ($p<0.0001$ for the polymer to TPP mass ratios of 3:1 and 5:1, $p<0.05$ for the polymer to TPP mass ratio of 4:1). Other studies reported the effect of the type of polymer on the size of the nanoparticles. For instance, Shahnaz et. al. [63] found that the size of thiolated chitosan nanoparticles was smaller than the size of unmodified chitosan nanoparticles. Similarly, Eliyahu et al. [64] found that the size of acrylated chitosan nanoparticles (with 65% degree of acrylation) was smaller than the size of unmodified chitosan nanoparticles which could be related to the decrease in the number of the free amino groups of acrylated chitosan available for crosslinking with TPP.

PDI of some of the MeCHI nanoparticles were relatively large (Table 1) which could be due to the difference in the polymer/TPP mass ratio used in their formulation. Additionally, grafting of chitosan with methacrylated groups increases the molecular weight of chitosan which could result in a slight increase in the PDI values. In general, PDI has values in the range of 0 to 1. Values greater than 0.7 indicate broad size distribution i.e. samples are polydisperse [65]. However, the MeCHI nanoparticles formulations which were selected for further studies had the PDI of around 0.4 which is acceptable.

3.3.3. Effect of NaCl addition

NaCl (0.5 mg/mL) was added to the formulations of chitosan and MeCHI nanoparticles and the resultant nanoparticles were evaluated in terms of their size and PDI. Jonassen, et.al. [58] reported that NaCl had a significant effect on the size and zeta potential of chitosan nanoparticles. As per the literature, the ionic strength of the medium also affects the charge density of chitosan nanoparticles and changes their conformation [66]. These conformational changes that are due to the intramolecular repulsive forces are significant in the solutions. Therefore, two polymer/TPP mass ratios (4:1 and 5:1) were used to explore the effects of NaCl on the size, PDI, and zeta potential of chitosan and MeCHI nanoparticles. For chitosan nanoparticles, it was found that at both 4:1 and 5:1 polymer to TPP mass ratios, the addition of NaCl did not make any significant difference ($p > 0.05$) in the particle size (Figure 4a). This is not consistent with the results published by Jonassen et al. [58] as they reported that the presence of NaCl led to a decrease in the size of the chitosan nanoparticles, which might be due to the differences in the concentration of NaCl used in the two studies. The difference in the molecular weight and the degree of deacetylation of the chitosan used in the preparation of the nanoparticles can be considered as the other important reasons for such observation. Also, Figure 4b shows that the addition of NaCl did not have any significant effects ($p > 0.05$) on the PDI of chitosan and MeCHI nanoparticles.

As expected, in the case of MeCHI nanoparticles, at a 4:1 polymer/TPP mass ratio, the addition of NaCl significantly increased the particle size ($p < 0.05$). No studies reported the effects of NaCl on the size of MeCHI nanoparticles, however, Sawtarie, et al. [67] observed similar effects on the size of unmodified chitosan-TPP nanoparticles at a specific concentration of NaCl. The increase in the size of MeCHI nanoparticles could be related to the two effects of NaCl on chitosan-TPP nanoparticles formation: (1) screening of electrostatic repulsion between the aggregating subunits of the nanoparticles, which increases their collision frequency and aggregation; and (2) competitive binding of chloride anions (Cl^-) and TPP anions, which weakens chitosan-TPP binding. Although the weakening of chitosan-TPP binding slows both particle formation and aggregation down, in the presence of NaCl, the aggregation process becomes faster relative to the primary particle formation and, consequently, more aggregation occurs before the free TPP is consumed by the process of primary particle formation and therefore larger nanoparticles will be formed [67].

3.3.4. Effect of TPP concentration

To investigate the effects of TPP concentration (1 mg/mL and 0.5 mg/mL) on the particle size and PDI, four formulations of each of chitosan and MeCHI nanoparticles were prepared at polymer to TPP mass ratios of 4:1 and 5:1 with and without NaCl. The results of these studies are shown in Figure 4. For chitosan nanoparticles, with and without NaCl, changing TPP concentration had no significant effect on the particle size and PDI. This is in agreement with the study of Fan et al. [68] who reported that TPP concentration below 1.5 mg/mL had no significant effect on the size and PDI of chitosan nanoparticles. For MeCHI nanoparticles, without NaCl, there was only a significant increase in particle size ($p < 0.01$) at both 4:1 and 5:1 polymer to TPP mass ratios with decreasing TPP concentration, but no significant change in PDI was observed. For MeCHI nanoparticles, a decrease in TPP concentration significantly increased ($p < 0.0001$) the particle size only when a 4:1 polymer/TPP mass ratio with NaCl, (Figures 4c, and 4d). This might be due to that at higher TPP concentrations, a higher cross-linking degree of the MeCHI nanoparticles can also be achieved which could result in a more compact particle structure. In contrast, at a 5:1 polymer to TPP mass ratio and in the presence of NaCl, a decrease in TPP concentration had no significant effect on the size and PDI of MeCHI nanoparticles.

3.3.5. Zeta potential

The value of the zeta potential of all the chitosan and MeCHI nanoparticles was positive which is due to the presence of protonated amino group (NH_3^+) of chitosan in the aqueous solutions. As shown in Table 1, both chitosan and MeCHI nanoparticles had the highest zeta potential at a 4:1 polymer/TPP mass ratio. The presence of NaCl (0.5 mg/mL) in both chitosan and MeCHI nanoparticles, at a 4:1 polymer/TPP mass ratio, led to a significant decrease in the zeta potential which could be due to the screening of the charge of the nanoparticles by the ions of NaCl [55].

For chitosan nanoparticles at a 4:1 chitosan/TPP mass ratio, with and without NaCl, the zeta potential was 9.10±0.52 mV and 12.50±0.26 mV, respectively. The zeta potential of MeCHI nanoparticles at 4:1 MeCHI /TPP mass ratio, with and without NaCl, was 10.33±1.59 mV and 10.85±0.07 mV, respectively. Also, the addition of NaCl at polymer/TPP mass ratio of 5:1 and 0.5 mg/mL TPP concentration had no significant effect on the zeta potential of the unmodified chitosan nanoparticles.

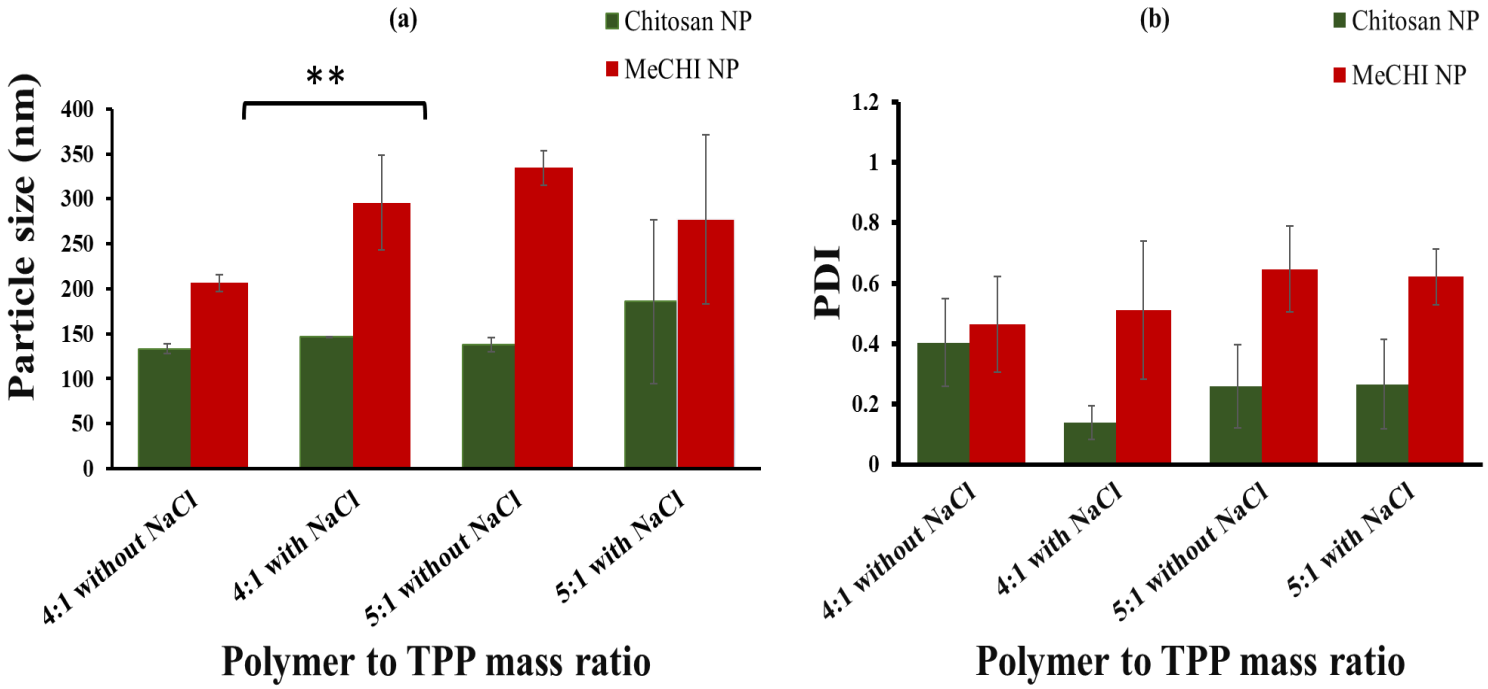

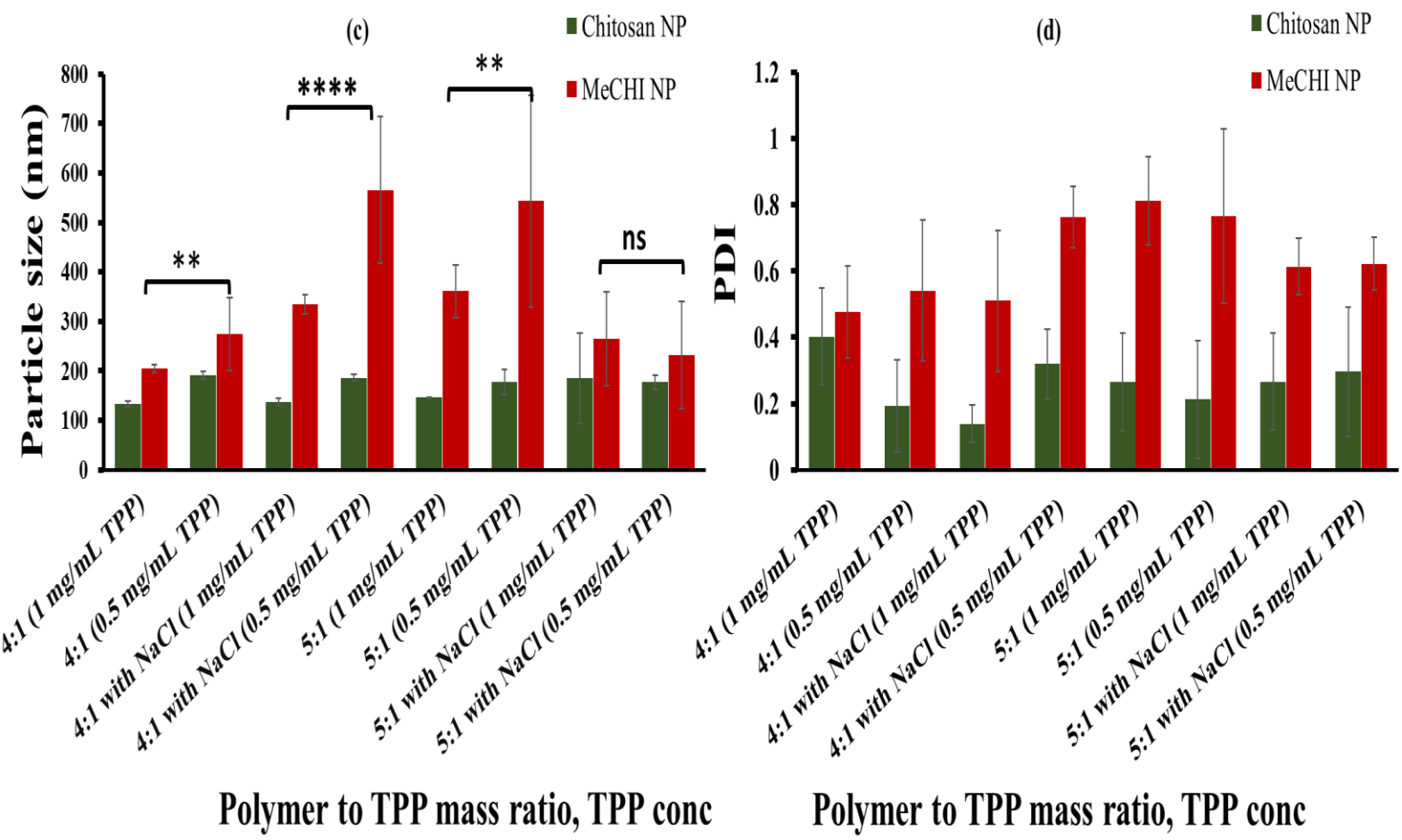

Figure 4. (a) Effects of NaCl on the mean particle size, (b) Effects of NaCl on PDI, (c) Effects of TPP concentration on mean particle size, and (d) Effects of TPP concentrations on PDI. (**): p<0.01, (****) p<0.0001, (*): p<0.05, (ns): not significant, NP nanoparticles

3.3.6. Preparation of ciprofloxacin-loaded chitosan and MeCHI nanoparticles

Figures S5 and S6 show the DLS size distributions of both unloaded and ciprofloxacin-loaded chitosan and MeCHI nanoparticles, respectively. Ciprofloxacin-loaded MeCHI nanoparticles (when 1 mg/mL TPP solution was used) showed a slightly broader particle size distribution compared to their unmodified chitosan counterpart. Table 2 shows the size, PDI, and zeta potential of the ciprofloxacin-loaded nanoparticles. Generally, the addition of ciprofloxacin led to an increase in the particle size which could be due to the presence of the negatively charged carboxylate anions (COO^-) in ciprofloxacin which reduces the interactions between TPP and

chitosan and this could eventually form particles with a low degree of compactness, low density yet more porosity and large particle size. Also, the addition of ciprofloxacin decreased the zeta potential of the nanoparticles. This is due to the presence of the negatively charged carboxylate anions (COO^-) in ciprofloxacin which neutralizes the positively charged amino groups of chitosan and MeCHI on the surface of the nanoparticles. Generally, ciprofloxacin-loaded unmodified chitosan nanoparticles had a smaller size ($p < 0.01$) than ciprofloxacin-loaded MeCHI nanoparticles which could be due to the less dense structure of the nanoparticles formed from MeCHI compared to unmodified chitosan. The presence of NaCl significantly decreased the size of ciprofloxacin-loaded unmodified chitosan nanoparticles. However, the TPP concentration had no significant effect on the size of ciprofloxacin-loaded MeCHI nanoparticles (Table 2).

Table 2. Physicochemical properties of ciprofloxacin-loaded chitosan and MeCHI nanoparticles at 4:1 polymer/TPP mass ratio (mean ± SD, n=3).

Formulation	TPP concentration (mg/mL)	Mean particle size (nm)	PDI	Z-average size (nm)	Zeta potential (mV)	EE (%)	LC (%)
CIP+Chitosan without NaCl	1	293 ± 93^{B}	0.333± 0.152	201±14	6.40±2.53	56 ± 13^{B}	14 ± 2^{B}
CIP+Chitosan with NaCl	1	161 ± 9^{A}	0.162± 0.078	154± 1	0.50±0.43	45 ± 17^{A}	9 ± 3^{A}
CIP+MeCHI without NaCl	1	384 ± 39^{B}	0.656± 0.251	395±90	10.03±0.90	54 ± 3^{A}	15 ± 2^{A}
CIP+MeCHI without NaCl	0.5	171 ± 10^{B}	0.556± 0.05	156±3	9.21±2.25	69 ± 13^{B}	16 ± 1^{A}

EE: encapsulation efficiency, LC: loading capacity, CIP: ciprofloxacin, MeCHI: methacrylated chitosan.
Superscripts; A indicates no statistical significant difference, B indicates statistical significant difference.

3.4. TEM Analysis

TEM micrographs show that both chitosan and MeCHI nanoparticles have a spherical shape and a smooth surface (Figure 5). From the TEM analysis, it was found that the size of unloaded chitosan and MeCHI nanoparticles was 32±8 nm and 15±12 nm, respectively. The size of ciprofloxacin-loaded chitosan and MeCHI nanoparticles was 11±3 nm, and 45±8 nm, respectively. The size obtained using TEM analysis was significantly smaller than the size obtained using DLS analysis. The DLS size of unloaded chitosan and MeCHI nanoparticles was 133±5 nm and 206±9 nm, respectively. The DLS size of ciprofloxacin-loaded chitosan and MeCHI nanoparticles was 293±93 nm and 384±39 nm, respectively. This discrepancy in the size of the nanoparticles is expected as DLS analysis was performed using nanoparticle suspensions in the fully hydrated and swollen state and thus larger size values could be obtained. However, in the TEM analysis, the samples were air-dried and dehydrated before the analysis. Several reports also corroborate the TEM results of the current study [69, 70].

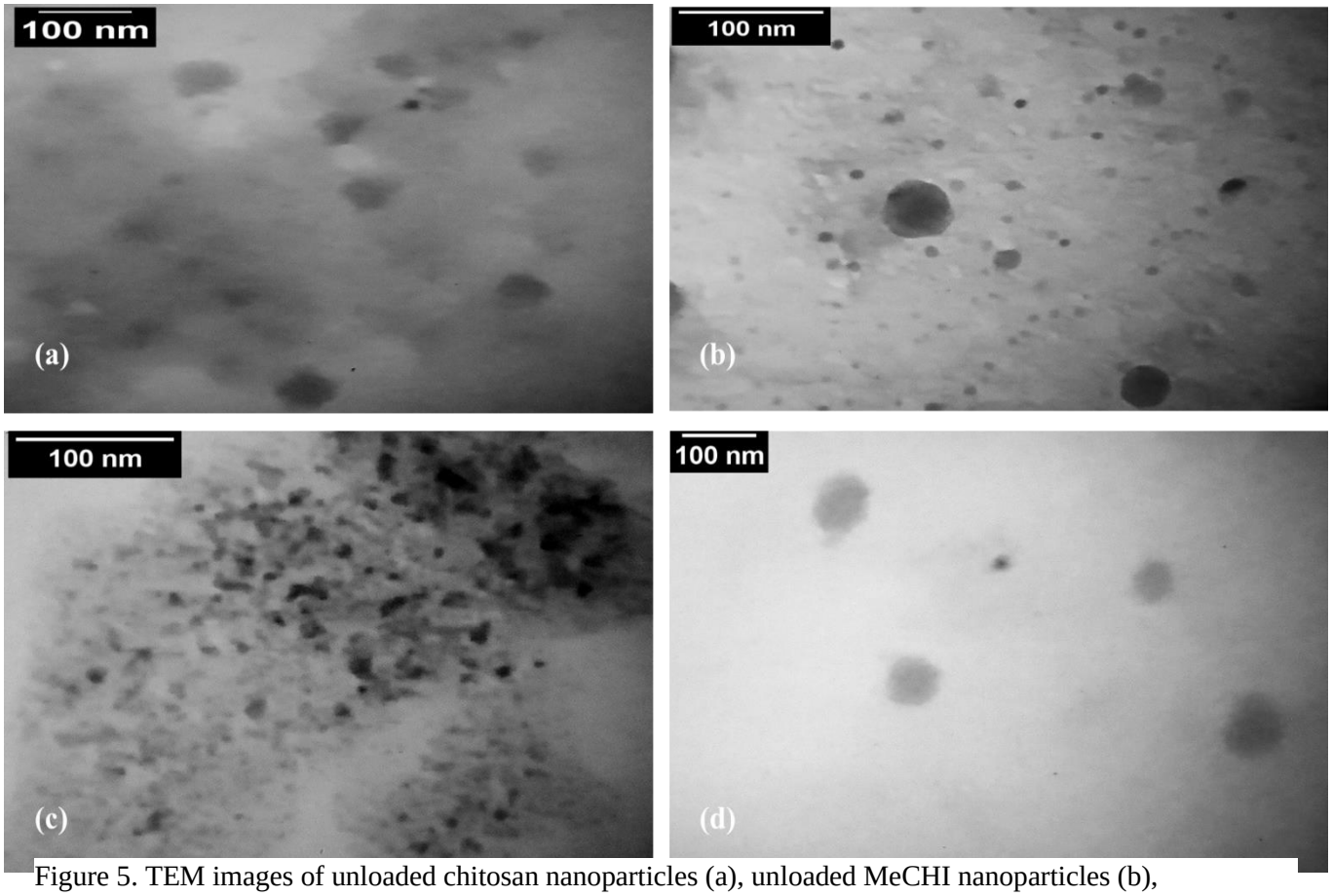

Figure 5. TEM images of unloaded chitosan nanoparticles (a), unloaded MeCHI nanoparticles (b), ciprofloxacin-loaded chitosan nanoparticles (c), and ciprofloxacin-loaded MeCHI nanoparticles (d).

3.5. EE and LC

Table 2 shows the EE and LC of ciprofloxacin-loaded chitosan and MeCHI nanoparticles. It is clear that the presence of NaCl in chitosan nanoparticles led to a decrease in EE and LC. This could be due to the competition of carboxylic groups of ciprofloxacin molecules with chloride anions (Cl^-) of NaCl for binding to the amino groups of chitosan which could decrease the electrostatic attractions between the positively charged protonated amino groups (NH_3^+) of chitosan and the negatively charged carboxylate groups of ciprofloxacin resulting in a EE of the drug. This result is consistent with the study of Binesh et al. [71] who observed that NaCl decreased the EE of metronidazole-loaded chitosan nanoparticles. On the other hand, decreasing the concentration of TPP from 1 mg/mL to 0.5 mg/mL led to a significant increase ($p < 0.0001$) in the EE of ciprofloxacin-loaded MeCHI nanoparticles, which could be attributed to the low degree of competition of ciprofloxacin molecules with TPP for binding to the polymer at low TPP concentration and therefore an increase in the number of binding sites of polymers available to interact with the drug.

3.6. Drug Release

Figure 6 shows the percentage of cumulative drug release from free ciprofloxacin solution, ciprofloxacin-loaded chitosan, and MeCHI nanoparticles within 48 hours. A bimodal drug release pattern was observed which includes an initial burst release of ciprofloxacin followed by a slow release. The initial burst release could be due to the release of the drug molecules which are adsorbed on the surface of the nanoparticles [72,73]. The subsequent slow drug release could be attributed to the release of the drug molecules which are entrapped by the nanoparticles. On the other hand, the free drug solution provided an immediate drug release where more than 80% of the drug was released in 75 minutes.

Drug release in simulated gastric fluid (pH 1.2, Figure 6a) shows that chitosan nanoparticles with NaCl have the greatest percentage of drug release. The cumulative drug release from the ciprofloxacin-loaded chitosan nanoparticles without NaCl and with NaCl after 48 hours was 24.8±1.9% and 26.7±1.7%, respectively. The cumulative drug release from ciprofloxacin-loaded MeCHI nanoparticles at 1 mg/mL and 0.5 mg/mL TPP concentrations after 48 hours was 16.6±1.5% and 18.3±0.4%, respectively.

Drug release in simulated intestinal fluid (pH 6.8, Figure 6b) shows that chitosan nanoparticles without NaCl have the greatest percentage of drug release. The cumulative drug release from the

ciprofloxacin-loaded chitosan nanoparticles without NaCl and with NaCl after 48 hours was 24.8±1.4% and 14.1±1.0%, respectively. For chitosan nanoparticles, the addition of NaCl significantly decreased ($p < 0.0001$) the percentage of cumulative drug release after 48 hours which could be due to the decrease in the zeta potential of these nanoparticles (Table 2), leading to the increase in the electrostatic attractions between chitosan macromolecules. This can result in a denser nanoparticles structure which could impede the diffusion of the drug and therefore a slower drug release. MeCHI nanoparticles showed a significantly smaller percentage of cumulative drug release ($p < 0.001$) after 48 hours compared to chitosan nanoparticles (both with 1 mg/mL TPP) which could be attributed to the relatively more hydrophobic nature of MeCHI compared to unmodified chitosan due to the presence of methacrylate groups which decreased the dissolution rate and swelling of MeCHI macromolecules [74]. Therefore, MeCHI nanoparticles provided a more prolonged or sustained drug release compared to the unmodified chitosan nanoparticles.

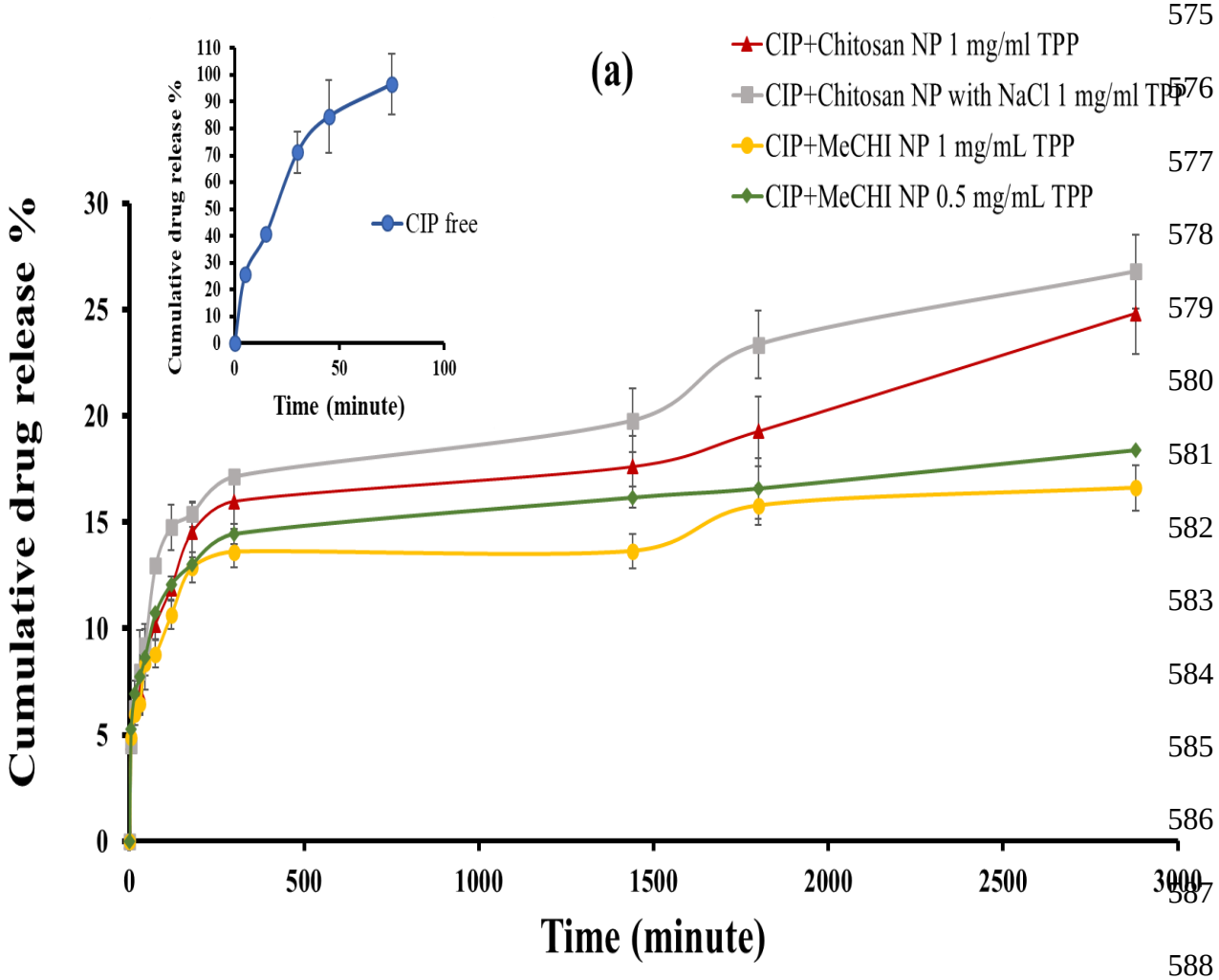

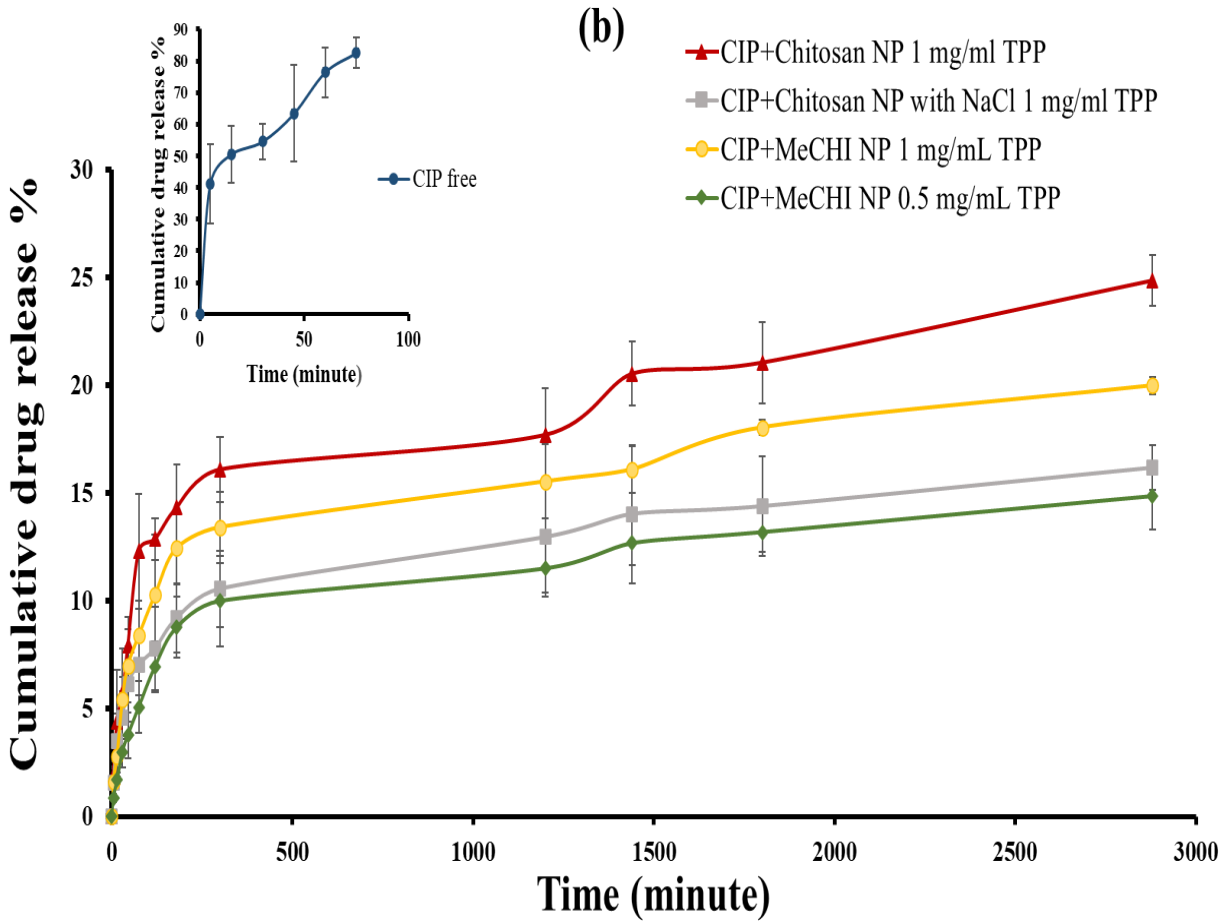

Figure 6. (a) Percentage of cumulative drug release of ciprofloxacin-loaded chitosan and MeCHI nanoparticles at pH (a) 1.2, and (b) 6.8. (a) MeCHI nanoparticles have more prolonged drug release compared to chitosan nanoparticles ($p<0.0001$). (b) MeCHI nanoparticles provided slower drug release ($p<0.001$) compared to unmodified chitosan nanoparticles. The insert shows the release from the free drug solution, CIP: ciprofloxacin, NP: nanoparticles.

The cumulative drug release from ciprofloxacin-loaded MeCHI nanoparticles at 1 mg/mL and 0.5 mg/mL TPP concentrations after 48 hours was 20.0±0.4% and 14.8±1.8%, respectively. Decreasing the concentration of TPP solution from 1 mg/mL to 0.5 mg/mL significantly decreased the percentage of cumulative drug release ($p<0.0001$) from ciprofloxacin-loaded MeCHI nanoparticles which could be due to the stronger interactions between ciprofloxacin and MeCHI

at low TPP concentration in simulated intestinal fluid. This is also consistent with the EE data (Table 2) as the decrease in TPP concentration resulted in a higher EE.

3.7. Mucoadhesion Study

The retention of ciprofloxacin-loaded chitosan and MeCHI nanoparticles on the sheep abomasum mucosa was evaluated. The sheep abomasum mucosa was selected as an ex vivo model to test the mucoadhesive properties of chitosan and MeCHI nanoparticles as the stomach is the first organ of the GIT, which is lined with mucosal surfaces, where the nanoparticles will reside for a prolonged period of time before their transit into the small intestine and colon.

A piece of sheep abomasum (the actual stomach of ruminants) was used. Abomasum has a similar function as the stomach of a non-ruminant which includes the secretion of enzymes and acids to break down nutrients [76]. There was a significant difference ($p<0.0001$) in the retention of free ciprofloxacin solution compared to all types of the tested ciprofloxacin-loaded chitosan and MeCHI nanoparticles. In the case of free ciprofloxacin solution, only 22±11% of the drug was retained on the sheep abomasum mucosa after washing with 20 mL simulated gastric fluid (Figure 7). However, the nanoparticles were able to adhere to the mucosal membrane of the abomasum and their retention was significantly higher than free ciprofloxacin solution. Even after extensive and 8 cycles of washing with 20 mL simulated gastric fluid, 87 to 96 % of the nanoparticles remained on the surface of the sheep abomasum mucosa. This is attributed to the mucoadhesive properties of chitosan owing to its ability to bind to the mucus layer of mucosa via hydrogen bonding, electrostatic attractions, and hydrophobic effects. Interestingly, there was a significant difference ($p<0.05$) in the percentage of nanoparticles that remained on the abomasum mucosa between ciprofloxacin-loaded chitosan nanoparticles without NaCl and ciprofloxacin-loaded MeCHI nanoparticles (with 1 mg/mL TPP and without NaCl) (88.0±6.9 % and 96.0±0.4 %, respectively) after a 20 mL wash off cycle. This indicated that ciprofloxacin-loaded MeCHI nanoparticles were significantly more mucoadhesive compared to the unmodified chitosan nanoparticles. Better mucosal retention of the ciprofloxacin-loaded MeCHI nanoparticles could be due to the enhanced mucoadhesivity of the MeCHI used in their formulation [36]. It is believed that MeCHI has a superior mucoadhesivity compared to the unmodified chitosan because of the

ability of MeCHI to bind to the mucus via covalent bonds between methacrylate groups of MeCHI and the thiol groups of the mucus components [36]. The increase in the hydrophobicity of MeCHI due to the introduction of hydrophobic methacrylate groups could also lead to stronger hydrophobic interactions between MeCHI nanoparticles and mucus components [36]. Additionally, the intrinsic properties of unmodified chitosan including hydrogen bonding and electrostatic attractions could still be preserved upon its chemical modification, but this hypothesis requires further investigation. On the other hand, when the concentration of TPP in MeCHI nanoparticles was decreased (from 1 mg/mL to 0.5 mg/mL), no significant difference in the retention of unmodified chitosan and MeCHI nanoparticles and the two different types of MeCHI nanoparticles was observed. These findings indicate that MeCHI nanoparticles are more mucoadhesive than unmodified chitosan nanoparticles when a particular TPP concentration (in this case high concentration) is used which could be due to the presence of high TPP concentration resulting in high ionic strength. This is consistent with previous studies which explored that the chitosan-mucin interactions, at low pH and high ionic strength, may involve other attractive forces such as hydrogen bonding and/or hydrophobic interactions, in addition to electrostatic interactions [77]. Therefore, optimization of MeCHI nanoparticles formulations is essential to enhance their mucoadhesivity as the type and concentration of the formulation excipients can have a significant effect on the mucoadhesivity of the nanoparticles. The enhanced mucoadhesivity can increase the residence time of drugs at the site of application and/or absorption and sustains its release which may enhance the drug absorption and bioavailability [78,79]. For antibiotics such as ciprofloxacin, better mucoadhesivity of the carrier nanoparticles can help in the treatment of different GIT diseases particularly gastritis and ulcers associated with H-pylori infection through the decreased frequency of administration and better patient compliance as well as the enhanced therapeutic activity. Additionally, MeCHI nanoparticles are expected to have better chemical stability compared to thiolated systems as the thiol groups in the thiolated systems could undergo oxidation which could result in the loss of mucoadhesive properties upon long-term storage [28].

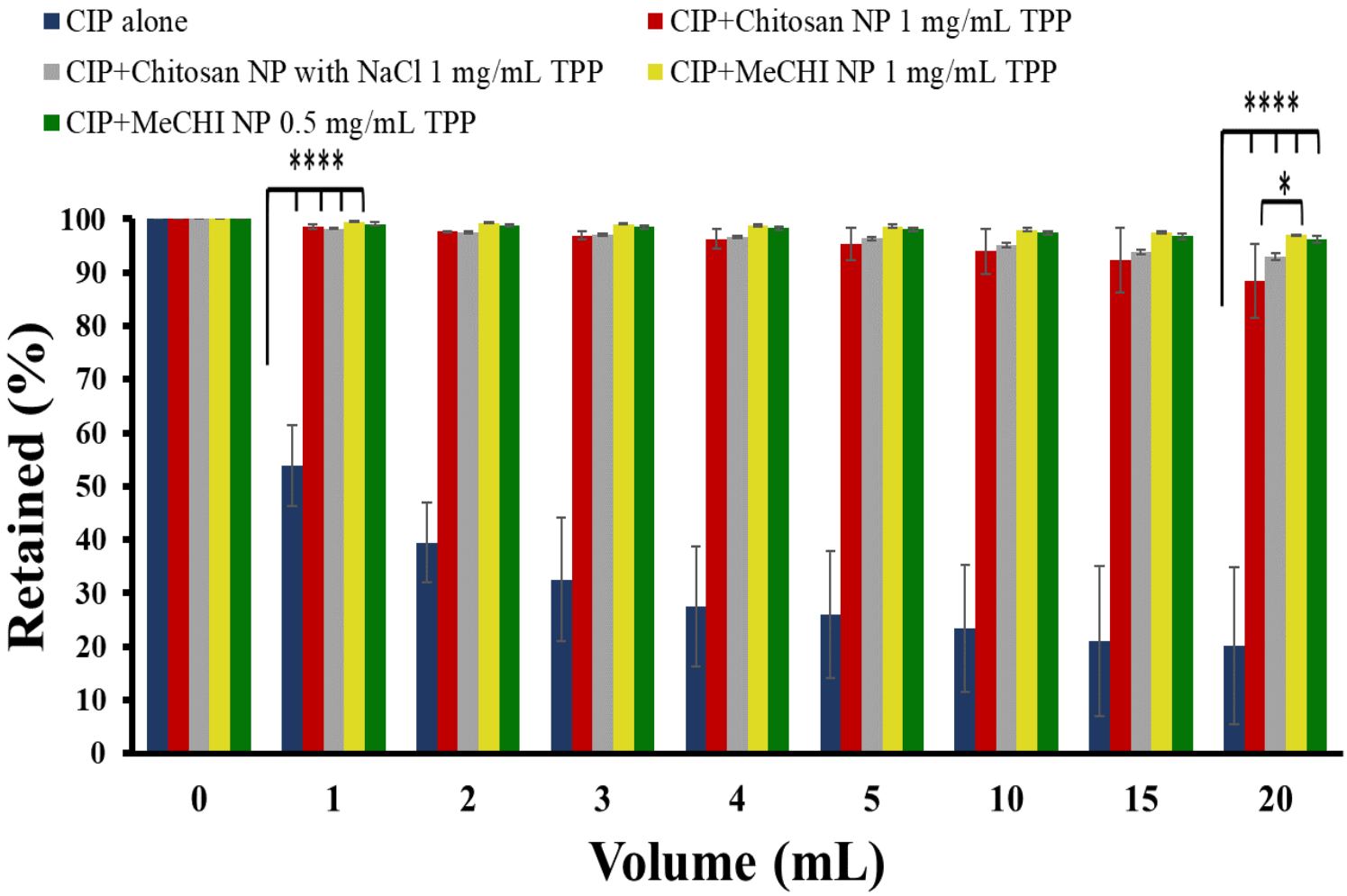

Figure 7. Retention of ciprofloxacin-loaded chitosan and MeCHI nanoparticles on sheep abomasum mucosa (mean ± SD, n=3). CIP: ciprofloxacin, NP: nanoparticles, (****) $p<0.0001$, (*): $p<0.05$.

3.8. Stability Studies

3.8.1. Storage stability study

To evaluate the storage stability of the nanoparticles, the general appearance of the ciprofloxacin-loaded chitosan and MeCHI nanoparticles was investigated for the presence of any precipitation and color change at 4 ºC and 25 ºC over a period of 6 months. After 2 months, chitosan nanoparticles underwent particle aggregation and precipitation at 25 ºC. After 4 months, in addition to the particle aggregation, the color of chitosan nanoparticles suspensions also changed from light blue to yellow. After 6 months, the color was changed again from yellow to light brown

(Figure S7) indicating the long-term instability of these nanoparticles at 25 ºC. The color change of the nanoparticles could be due to their aggregation and possible degradation, but further investigations including the chemical analysis are required to understand these observations. In contrast, MeCHI nanoparticles did not show any color change over 6 months, but only a slight aggregation was observed after 2 and 4 months, and precipitation after 6 months. The general appearance of both chitosan and MeCHI nanoparticles remained unchanged when stored at 4 ºC for 6 months. The results were consistent with Haliza Katas et al., [80] who reported that chitosan nanoparticles should not be stored at ambient temperature as they could undergo degradation due to an increase in the kinetic movement of the nanoparticles.

Therefore, the size and PDI of the nanoparticles were analyzed after storing the nanoparticles in a fridge at 4 ºC for 6 months. As shown in Table 3, only a slight change in the size of the nanoparticles was observed, although the size was still below 305 nm. The size of ciprofloxacin-loaded chitosan nanoparticles (with and without NaCl) and MeCHI nanoparticles (0.5 mg/mL TPP) significantly increased which may be attributed to the aggregation of the individual nanoparticles and hydration and swelling of the nanoparticles in the presence of water [81,82]. The results are consistent with the study of Haliza Katas et al, [80] who observed a slight increase in the size of chitosan nanoparticles only after 14 days of storage at 4ºC. It is worth mentioning that after 6 months of storage, only 9% increase in the size of the nanoparticles was observed. However, the size of ciprofloxacin-loaded MeCHI nanoparticles (with 1 mg/mL TPP) significantly decreased which could be due to the dissolution of some of the larger nanoparticles [82]. This reduction in particle size is consistent with the study of Min-Lang Tsai et al., [81] who studied unmodified chitosan nanoparticles, and revealed that the formulations of initially larger size became smaller upon storage for 10 days, while those of initially smaller size became larger. Overall ciprofloxacin-loaded MeCHI nanoparticles were more stable than their chitosan counterparts. No significant change in the PDI of ciprofloxacin-loaded chitosan nanoparticles (with and without NaCl) and MeCHI nanoparticles (with 0.5 mg/mL TPP) was observed. However, the PDI of MeCHI nanoparticles (with 1 mg/mL TPP) significantly decreased ($P<0.001$).

Table 3. Stability profiles of ciprofloxacin-loaded chitosan and MeCHI nanoparticles after storage for 6 months at 4 ºC, in stimulated gastric fluid (pH 1.2) and simulated intestinal fluid (pH 6.8) (mean ± SD, n=3).

	Particle size (nm)				PDI			
Formulation	**Freshly prepared pH 5**	**Stored for 6 months**	**pH 1.2**	**pH 6.8**	**Freshly prepared in pH 5**	**Stored for 6 months**	**pH 1.2**	**pH 6.8**
CIP+Chitosan without NaCl	293±93	305±2	287±60	123±8	0.182±0.078	0.364±0.166	0.622±0.246	0.616±0.029
CIP+Chitosan with NaCl	161±9	289±12	178±10	155±15	0.335±0.152	0.291±0.082	0.504±0.217	0.626±0.019
CIP+MeCHI without NaCl (1 mg/mL TPP)	384±39	264±10	196±11	253±16	0.556± 0.05	0.221±0.055	0.634±0.026	0.599±0.027
CIP+MeCHI without NaCl (0.5 mg/mL TPP)	171± 10	195±2	186±15	201±15	0.65± 0.251	0.632±0.178	0.656±0.038	0.64±0.071

3.9.2. pH stability study

The stability of nanoparticles *in vitro* is important to predict the stability of nanoparticles in the human body fluids including gastric and intestinal fluids. The prepared ciprofloxacin-loaded chitosan and MeCHI nanoparticles were placed in simulated gastric and intestinal fluids and their size and PDI were measured and compared to their initial values. Some differences were observed, however, the size and PDI were still lower than 300 nm and 0.7, respectively (Table 3) and this indicates the acceptable physical stability of the nanoparticles in simulated gastric and intestinal fluids.

In simulated gastric fluid, no significant change in the size of chitosan nanoparticles (with and without NaCl) and MeCHI nanoparticles (with 0.5 mg/mL TPP) was observed. In contrast, the size of MeCHI nanoparticles (with 1 mg/mL TPP) significantly decreased ($p<0.0001$) which could be due to the increase in the hydronium ion concentration which could attract the negatively charged

TPP molecules, competing with MeCHI macromolecules and weaken the electrostatic attractions between MeCHI and TPP. This interaction could be more significant in a higher TPP concentration. PDI of the chitosan nanoparticles with and without NaCl significantly increased. However, no significant change in the PDI of MeCHI nanoparticles was observed.

In simulated intestinal fluid, the size of chitosan (with and without NaCl) and MeCHI nanoparticles (1 mg/mL TPP) significantly decreased which could be due to the collapse of the swollen polymer chains caused by deprotonation of the amino groups of chitosan and MeCHI [83]. However, no significant change in the size of MeCHI nanoparticles (0.5 mg/mL TPP) was observed. PDI of chitosan nanoparticles (with and without NaCl) significantly increased. In contrast, similar to the simulated gastric fluid, no significant change in the PDI of MeCHI nanoparticles in the simulated intestinal fluid was observed.

4. Conclusions

The mucoadhesive chitosan and MeCHI nanoparticles were fabricated using an ionic cross-linking method. Optimization of nanoparticles formulations explored the effects of polymer/TPP mass ratio, the TPP concentration and the presence of NaCl on the size, polydispersity and zeta potential of unmodified chitosan and MeCHI nanoparticles. It was found that the smallest MeCHI nanoparticles with a relatively low PDI can be prepared using polymer/TPP mass ratio of 4:1. Unloaded and ciprofloxacin-loaded MeCHI nanoparticles were larger than unmodified chitosan nanoparticles. No significant difference in the PDI of chitosan and MeCHI nanoparticles at 4:1 polymer/TPP mass ratio was observed. EE of ciprofloxacin-loaded MeCHI nanoparticles can be increased by decreasing TPP concentration. Ciprofloxacin-loaded MeCHI nanoparticles provided a slower and more sustained drug release compared to their chitosan counterpart. Both ciprofloxacin-loaded chitosan and MeCHI nanoparticles showed stronger retention on the sheep abomasum mucosa compared to the free ciprofloxacin solution. However, ciprofloxacin-loaded MeCHI nanoparticles with optimum TPP concentration showed superior *ex vivo* mucoadhesivity than its unmodified chitosan counterpart. The *in vivo* mucoadhesive properties of these MeCHI nanoparticles could potentially be investigated using animal models in the future. MeCHI nanoparticles can be considered as promising drug delivery systems due to their mucoadhesive and controlled drug release properties as well as improved stability profiles.

Acknowledgments: The authors acknowledge the College of Pharmacy, University of Sulaimani for their support in conducting this study. The authors are grateful to the University of Reading for providing NMR and FTIR facilities. The authors thank Pioneer Co. for Pharmaceutical Industries (Kurdistan Region, Iraq) for the facilities used in the chemical analysis.

References

1. AA Elzatahry, MM Eldin, Preparation and characterization of metronidazole-loaded chitosan nanoparticles for drug delivery application, Polym. Adv. Technol. 19 (2008) 1787-1791. https://doi.org/10.1002/pat.1195

2. A Bernkop-Schnürch, Mucoadhesive systems in oral drug delivery, Drug Discov Today Technol. 2 (2005) 83-87. https://doi.org/10.1016/j.ddtec.2005.05.001

3. K Zhao, Y Xie, X Lin, W Xu, The mucoadhesive nanoparticle-Based delivery system in the development of mucosal vaccines. Int J Nanomedicine. 17 (2022) 4579-4598 https://doi.org/10.2147/IJN.S359118

4. R Cazorla-Luna, A Martín-Illana, F Notario-Pérez, R Ruiz-Caro, M-D Veiga, Naturally Occurring Polyelectrolytes and Their Use for the Development of Complex-Based Mucoadhesive Drug Delivery Systems: An Overview, Polymers. 13 (2021) 2241. https://doi.org/10.3390/polym13142241

5. FD Rajput GC, Majmudar, JK Patel, Patel KN, RS Thakor, BP Patel, NB Rajgor, Stomach specific mucoadhesive tablets as controlled drug delivery system–A review work, Int. J. Pharm. Biol. Res. 1 (2010) 30-41.

6. AR Shirvan, A Bashari, N Hemmatinejad, New insight into the fabrication of smart mucoadhesive buccal patches as a novel controlled-drug delivery system, Eur. Polym. J. 119 (2019) 541-550. https://doi.org/ 10.1016/j.eurpolymj.2019.07.010

7. R Yahagi, Y Machida, H Onishi, Mucoadhesive suppositories of ramosetron hydrochloride utilizing Carbopol®, Int. J. Pharm. 193 (2000) 205-212. https://doi.org/ 10.1016/S0378-5173(99)00338-5

8. F Acarturk, Mucoadhesive vaginal drug delivery systems, Recent Pat. Drug. Deliv. Formul. 3 (2009) 193-205. https://doi.org/10.2174/187221109789105658

9. I Pilipenko, V Korzhikov-Vlakh, A Valtari, Y Anufrikov, S Kalinin, M Ruponen, M Krasavin, A Urtti, T Tennikova, Mucoadhesive properties of nanogels based on stimuli-sensitive glycosaminoglycan-graft-pNIPAAm copolymers, Int. J. Biol. Macromol. 186 (2021) 864-872. https://doi.org/10.1016/j.ijbiomac.2021.07.070

10. PR Karn, Z Vanić, I Pepić, N Škalko-Basnet, Mucoadhesive liposomal delivery systems: the choice of coating material, Drug. Dev. Ind. Pharm. 37 (2011) 482-488. https://doi.org/10.3109/03639045.2010.523425

11. M Kannavou, K Karali, T Katsila, E Siapi, A Marazioti, P Klepetsanis, T Calogeropoulou, I Charalampopoulos, SG Antimisiaris, Development and comparative In vitro and In vivo study of BNN27 mucoadhesive liposomes and nanoemulsions for nose-to-brain delivery. Pharmaceutics, 15 (2023) 419. https://doi.org/10.3390/pharmaceutics15020419

12. K Sachan Nikhil, A Bhattacharya, Basics and therapeutic potential of oral mucoadhesive microparticulate drug delivery systems, Int. J. Pharm. Clin. 1 (2009) 10-14.

13. MA Mumuni, FC Kenechukwu, KC Ofokansi, AA Attama, DD Díaz, Insulin-loaded mucoadhesive nanoparticles based on mucin-chitosan complexes for oral delivery and diabetes treatment, Carbohydr. Polym. 229 (2020) 115506. https://doi.org/10.1016/j.carbpol.2019.115506

14. AJ Coutinho, SA Lima, CM Afonso, S Reis, Mucoadhesive and pH responsive fucoidan-chitosan nanoparticles for the oral delivery of methotrexate, Int. J. Biol. Macromol. 158 (2020) 180-188. DOI: 10.1016/j.ijbiomac.2020.04.233

15. IS Bayer, Recent advances in mucoadhesive interface materials, mucoadhesion characterization, and technologies, Adv. Mater. Interfaces. 9 (2022) 2200211. https://doi.org/10.1002/admi.2022002111`1qw2

16. T Wang, E Fleming, Y Luo, An overview of the biochemistry, synthesis, modification, and evaluation of mucoadhesive polymeric nanoparticles for oral delivery of bioactive compounds, Adv. Compos. Mater. 6 (2023) 6. https://doi.org/10.1007/s42114-022-00586-0

17. P Ramalingam, SW Yoo, YT Ko, Nanodelivery systems based on mucoadhesive polymer coated solid lipid nanoparticles to improve the oral intake of food curcumin, Food. Res. Int. 84 (2016) 113-119. https://doi.org/10.1016/j.foodres.2016.03.031

18. Z Yang, DJ McClements, X Peng, Z Xu, M Meng, L Chen, Z Jin, Fabrication of zein–carboxymethyl cellulose nanoparticles for co-delivery of quercetin and resveratrol, J. Food Eng. 341 (2023) 111322. https://doi.org/10.1016/j.jfoodeng.2022.111322

19. Y Wang, H Li, L Wang, J Han, Y Yang, T Fu, H Qiao, Z Wang, J Li, Mucoadhesive nanocrystal-in-microspheres with high drug loading capacity for bioavailability enhancement of silybin, Colloids Surf. B. 198 (2021) 111461. https://doi.org/10.1016/j.colsurfb.2020.111461

20. DA Subramanian, R Langer, G Traverso. Mucus interaction to improve gastrointestinal retention and pharmacokinetics of orally administered nano-drug delivery systems, J. Nanobiotechnology. 20 (2022) 1-23.

21. B Fan, L Liu, Y Zheng, Y Xing, W Shen, Q Li, R Wang, G Liang, Novel pH-responsive and mucoadhesive chitosan-based nanoparticles for oral delivery of low molecular weight heparin with enhanced bioavailability and anticoagulant effect, J. Drug Deliv. Sci. Technol. 78 (2022) 103955. https://doi.org/10.1016/j.jddst.2022.103955

22. R Rathi, Sanshita, A Kumar, V Vishvakarma, K Huanbutta, I Singh, T Sangnim. Advancements in Rectal Drug Delivery Systems: Clinical Trials, and Patents Perspective. Pharmaceutics. 14 (2022) 2210. https://doi.org/10.3390/pharmaceutics14102210

23. RH Costa, AP Krawczyk-Santos, JF Andrade, GN Barbalho, RM Almeida, YK Nóbrega, M Cunha-Filho, GM Gelfuso, SF Taveira, T Gratieri, α-Cyclodextrin-based poly (pseudo) rotaxane for antifungal drug delivery to the vaginal mucosa, Carbohydr. Polym.. 302 (2023) 120420. https://doi.org/ /10.1016/j.carbpol.2022.120420

24. S, I Khan, J Pandit, NA Emad, S Bano, KI Dar, MM Rizvi, MD Ansari, M Aqil, Y Sultana, Brain targeted delivery of carmustine using chitosan coated nanoparticles via nasal route for glioblastoma treatment, Int. J. Biol Ahmad. Macromo. 221 (2022) 435-4 45. https://doi.org/10.1016/j.ijbiomac.2022.08.210

25. M Saha, DR Saha, T Ulhosna SM, Sharker, MH Shohag, MS Islam, SK Ray, GS Rahman, HM Reza, QbD based development of resveratrol-loaded mucoadhesive lecithin/chitosan nanoparticles for prolonged ocular drug delivery, J. Drug Deliv. Sci. Technol. 63 (2021) 102480. https://doi.org/ 10.1016/j.jddst.2021.102480

26. X Gao, Y Xiong, H Chen, X Gao, J Dai, Y Zhang, W Zou, Y Gao, Z Jiang, B Han, Mucus adhesion vs. mucus penetration? Screening nanomaterials for nasal inhalation by MD simulation, J. Control. Release. 353 (2023) 366-379. https://doi.org/10.1007/s42114-022-00586-0

27. NA Hanafy, MA El-Kemary, Silymarin/curcumin loaded albumin nanoparticles coated by chitosan as muco-inhalable delivery system observing anti-inflammatory and anti COVID-19 characterizations in oleic acid triggered lung injury and in vitro COVID-19 experiment, Int. J. Biol. Macromol. 198 (2022) 101-110. https://doi.org/10.1016/j.ijbiomac.2021.12.073

28. TM M. Ways, WM Lau, VV Khutoryanskiy, Chitosan and its derivatives for application in mucoadhesive drug delivery systems, Polymers. 10 (2018) 267. https://doi.org/ 10.3390/polym10030267

29. KK Vandera, C Pague, J Omar, G González-Gaitano, TM Ways, VV Khutoryanskiy, CA Dreiss, Formation of Supramolecular Gels from Host–Guest Interactions between PEGylated Chitosan and α-Cyclodextrin, Macromol. Mater. Eng. (2023) 2200646. https://doi.org/10.1002/mame.202200646

30. IA Sogias, AC Williams, VV Khutoryanskiy, Why is chitosan mucoadhesive?, Biomacromolecules. 9 (2008) 1837-1842. https://doi.org/10.1021/bm800276d

31. I Bravo-Osuna, C Vauthier, A Farabollini, GF Palmieri, G Ponchel, Mucoadhesion mechanism of chitosan and thiolated chitosan-poly (isobutyl cyanoacrylate) core-shell nanoparticles, Biomaterials. 2007;28(13):2233-43. https://doi.org/10.1016/j.biomaterials.2007.01.005

32. TE Leonard, AF Liko, M Gustiananda, AB Putra AB, Juanssilfero, P Hartrianti, Thiolated pectin-chitosan composites: Potential mucoadhesive drug delivery system with selective cytotoxicity towards colorectal cancer, Int. J. Biol. Macromol. . 225 (2023) 1-2. https://doi.org/10.1016/j.ijbiomac.2022.12.012

33. E Meng-Lund, C Muff-Westergaard, C Sander, P Madelung, J Jacobsen, A mechanistic based approach for enhancing buccal mucoadhesion of chitosan, Int. J. Pharm. 416 (2014);280-285. https://doi.org/10.1016/j.ijpharm.2013.10.047

34. M Konovalova, B Shagdarova, A Zubareva, A Generalov, M Grechikhina, E Svirshchevskaya, Development of mucoadhesive chitosan-based drug delivery system, Prog. Chem. Appl. Chitin Deriv. 23 (2018) 103-113.

35. EE Hassan, JM Gallo, A simple rheological method for the in vitro assessment of mucin-polymer bioadhesive bond strength, Pharm. Res. 7 (1990) 491-495. https://doi.org/10.1023/A:1015812615635

36. OM Kolawole, WM Lau, VV Khutoryanskiy, Methacrylated chitosan as a polymer with enhanced mucoadhesive properties for transmucosal drug delivery, Int. J. Pharm. 550 (2018) 123-129. https://doi.org/10.1016/j.ijpharm.2018.08.034

37. A Bernkop-Schnurch, MH Hoffer, K Kafedjiiski, AH Krauland, Synthesis and in vitro evaluation of a novel thiolated chitosan. Biomaterials, 26 (2005); 819-826. https://doi.org/10.1016/j.biomaterials.2004.03.011

38. OM Kolawole, WM Lau, VV Khutoryanskiy, Synthesis and evaluation of boronated chitosan as a mucoadhesive polymer for intravesical drug delivery, J. Pharm. Sci. 108 (2019) 3046-3053. https://doi.org/10.1016/j.xphs.2019.05.006

39. Y Shitrit, H Bianco-Peled, Acrylated chitosan for mucoadhesive drug delivery systems, Int. J. Pharm. 517 (2017) 247-255. https://doi.org/10.1016/j.ijpharm.2016.12.023

40. LM Ferreira, AM Dos Santos, Boni FI, KC Dos Santos, LM Robusti, MP de Souza, NN Ferreira, SG Carvalho, VM Cardoso, M Chorilli, BS Cury, Design of chitosan-based particle systems: A review of the physicochemical foundations for tailored properties, Carbohydr. Polym.. 250 (2020) 116968. https://doi.org/10.1016/j.carbpol.2020.116968

41. J Potaś, E Szymańska, K Winnicka, Challenges in developing of chitosan–based polyelectrolyte complexes as a platform for mucosal and skin drug delivery, Eur. Polym. J. 140 (2020) 110020. https://doi.org/10.1016/j.eurpolymj.2020.110020

42. Y Luo, Q Wang, Recent development of chitosan-based polyelectrolyte complexes with natural polysaccharides for drug delivery, Int. J. Biol. Macromol. 64 (2014) 353-367. https://doi.org/10.1016/j.ijbiomac.2013.12.017

43. D Wu, L Zhu, Y Li, X Zhang, S Xu, G Yang, T Delair, Chitosan-based colloidal polyelectrolyte complexes for drug delivery: a review, Carbohydr. Polym. 238 (2020) 116126. https://doi.org/10.1016/j.carbpol.2020.116126

44. MK Amin, JS Boateng, Enhancing Stability and Mucoadhesive Properties of Chitosan Nanoparticles by Surface Modification with Sodium Alginate and Polyethylene Glycol for Potential Oral Mucosa Vaccine Delivery, *Mar. Drugs*. 20 (2022) 156. https://doi.org/10.3390/md20030156

45. MA Mohammed, JT Syeda, KM Wasan, EK Wasan, An overview of chitosan nanoparticles and its application in non-parenteral drug delivery, Pharmaceutics. 9 (2017) 53.

46. P Calvo, C Remunan-Lopez, JL Vila-Jato, MJ Alonso, Novel hydrophilic chitosan-polyethylene oxide nanoparticles as protein carriers, Appl. Polym. Sci. 63 (1997) 125-132. https://doi.org/ 10.1002/(SICI)1097-4628(19970103)63:1<125::AID-APP13>3.0.CO;2-4

47. TM Ways, SK Filippov, S Maji, M Glassner, M Cegłowski R, Hoogenboom, S King, WM Lau, VV Khutoryanskiy, Mucus-penetrating nanoparticles based on chitosan grafted with various non-ionic polymers: Synthesis, structural characterisation and diffusion studies, J. Colloid. Interface. Sci. 626 (2022) 251-264. https://doi.org/10.1016/j.jcis.2022.06.126

48. A Aburub, DS Risley, D Mishra, A critical evaluation of fasted state simulating gastric fluid (FaSSGF) that contains sodium lauryl sulfate and proposal of a modified recipe, Int. J. Pharm. 347 (2008) 16-22. https://doi.org/10.1016/j.ijpharm.2007.06.018

49. C Hasçiçek, N Gönül, N Erk, Mucoadhesive microspheres containing gentamicin sulfate for nasal administration: preparation and in vitro characterization, Farmaco. 58 (2003) 11-16. https://doi.org/ 10.1016/S0014-827X(02)00004-6

50. C Pornpitchanarong, T Rojanarata, P Opanasopit, T Ngawhirunpat, M Bradley, P Patrojanasophon, Maleimide-functionalized carboxymethyl cellulose: A novel mucoadhesive polymer for transmucosal drug delivery, Carbohydr. Polym. 288 (2022) 119368. https://doi.org/10.1016/j.carbpol.2022.119368

51. SM Bhagyaraj, OS Oluwafemi, Nanotechnology: the science of the invisible, In Synthesis of inorganic nanomaterials, (2018) 1-18. Woodhead Publishing. https://doi.org/10.1016/B978-0-08-101975-7.00001-4

52. A Adewuyi, WJ Lau, Nanomaterial development and its applications for emerging pollutant removal in water, In Handbook of nanotechnology applications (2021) pp. 67-97. Elsevier. https://doi.org/10.1016/B978-0-12-821506-7.00003-X

53. XZ Shu, KJ Zhu, The influence of multivalent phosphate structure on the properties of ionically cross-linked chitosan films for controlled drug release, Eur. J. Pharm. Biopharm. 54 (2002) 235-243. https://doi.org/10.1016/S0939-6411(02)00052-8

54. M Shafiei H, Jafarizadeh-Malmiri, M Rezaei, Biological activities of chitosan and prepared chitosan-tripolyphosphate nanoparticles using ionic gelation method against various pathogenic bacteria and fungi strains, Biologia. 74 (2019) 1561-1568. https://doi.org/10.2478/s11756-019-00299-8

55. J Antoniou, F Liu, H Majeed, J Qi, W Yokoyama, F Zhong, Physicochemical and morphological properties of size-controlled chitosan–tripolyphosphate nanoparticles, Colloids Surf, A Physicochem. Eng. Asp. 465 (2015) 137-146. https://doi.org/10.1016/j.colsurfa.2014.10.040

56. R Nunes, AS Serra, A Simaite, Â Sousa. Modulation of chitosan-TPP nanoparticle properties for plasmid DNA vaccines delivery. Polymers. 14 (2022) 1443. https://doi.org/10.3390%2Fpolym14071443

57. Malvern Panalytical**.** FAQ: Peak size or z-average size – which one to pick in DLS?: available online https://www.materials-talks.com/faq-peak-size-or-z-average-size-which-one-to-pick-in-dls/:(2023)

58. H Jonassen, AL Kjøniksen, M Hiorth, Stability of chitosan nanoparticles cross-linked with tripolyphosphate, Biomacromolecules. 13 (2012) 3747-3756. https://doi.org/10.1021/bm301207a

59. Malvern Panalytical. Dynamic light scattering - common terms defined: available online https://www.malvernpanalytical.com/en/learn/knowledge-center/whitepapers/wp111214dlstermsdefined:(2023)

60. AM Omer, ZM Ziora, TM Tamer, RE Khalifa, MA Hassan, MS Mohy-Eldin, MAT Blaskovich, Formulation of quaternized aminated chitosan nanoparticles for efficient encapsulation and slow release of curcumin. Molecules. 26 (2021) 449. https://doi.org/10.3390/molecules26020449

61. TM Tamer, MM ElTantawy, A Brussevich, A Nebalueva, A Novikov, IV Moskalenko, MM Abu-Serie, MA Hassan, S Ulasevich, EV Skorb, Functionalization of chitosan with poly aromatic hydroxyl molecules for improving its antibacterial and antioxidant properties: Practical and theoretical studies, Int. J. Biol. Macromol. 234 (2023) 123687. https://doi.org/10.1016/j.ijbiomac.2023.123687

62. MA Hassan, TM Tamer, AM Omer, WM Baset, E Abbas, MS Mohy-Eldin. Therapeutic potential of two formulated novel chitosan derivatives with prominent antimicrobial activities against virulent microorganisms and safe profiles toward fibroblast cells. Int. J. Pharm. 634 (2023) 122649. https://doi.org/10.1016/j.ijpharm.2023.122649

63. G Shahnaz, A Vetter, J Barthelmes, D Rahmat, F Laffleur, J Iqbal, G Perera, W Schlocker, S Dünnhaput, P Augustijns, A Bernkop-Schnürch. Thiolated chitosan nanoparticles for the nasal administration of leuprolide: bioavailability and pharmacokinetic characterization, Int. J. Pharm. 428 (2012) 164-170. https://doi.org/10.1016/j.ijpharm.2012.02.044

64. S Eliyahu, A Aharon, H Bianco-Peled. Acrylated chitosan nanoparticles with enhanced mucoadhesion. Polymers. 10 (2018) 106. https://doi.org/10.3390/polym10020106

65. H Zhang, M Oh, C Allen, E Kumacheva, Monodisperse chitosan nanoparticles for mucosal drug delivery, Biomacromolecules. 5 (2004) 2461-2468. https://doi.org/10.1021/bm0496211

66. TU Wani, AH Pandith, FA Sheikh, Polyelectrolytic nature of chitosan: Influence on physicochemical properties and synthesis of nanoparticles, J. Drug. Deliv. Sci. Technol . 65 (2021) 102730. https://doi.org/10.1016/j.jddst.2021.102730

67. N Sawtarie, Y Cai, Y Lapitsky, Preparation of chitosan/tripolyphosphate nanoparticles with highly tunable size and low polydispersity, Colloids Surf. B. 157 (2017) 110-117. https://doi.org/10.1016/j.colsurfb.2017.05.055

68. W Fan, W Yan, Z Xu, H Ni. Formation mechanism of monodisperse, low molecular weight chitosan nanoparticles by ionic gelation technique, Colloids Surf. B. 90 (2012) 21-27. https://doi.org/10.1016/j.colsurfb.2011.09.042

69. TM Ways, WM Lau, KW Ng, VV Khutoryanskiy, Synthesis of thiolated, PEGylated and POZylated silica nanoparticles and evaluation of their retention on rat intestinal mucosa in vitro, Eur. J. Pharm. Sci. 122 (2018) 230-238. https://doi.org/10.1016/j.ejps.2018.06.032

70. F Caputo, A Arnould, M Bacia, WL Ling, E Rustique, I Texier, AP Mello, AC Couffin, Measuring particle size distribution by asymmetric flow field flow fractionation: a powerful method for the preclinical characterization of lipid-based nanoparticles, Mol. Pharm. 16 (2019) 756-767. https://doi.org/10.1021/acs.molpharmaceut.8b01033

71. N Binesh, N Farhadian A, Mohammadzadeh, Enhanced antibacterial activity of uniform and stable chitosan nanoparticles containing metronidazole against anaerobic bacterium of Bacteroides fragilis, Colloids. Surf. B. 202 (2021) 111691. https://doi.org/10.1016/j.colsurfb.2021.111691Get

72. LH Chuah, N Billa, CJ Roberts, JC Burley, S Manickam, Curcumin-containing chitosan nanoparticles as a potential mucoadhesive delivery system to the colon. Pharm. Dev. Technol. 18 (2013) 591-599. https://doi.org/10.3109/10837450.2011.640688

73. J Yoo, YY Won, Phenomenology of the initial burst release of drugs from PLGA microparticles. ACS Biomater, Sci. Eng. 6 (2020) 6053-6062. https://doi.org/10.1021/acsbiomaterials.0c01228

74. KC Petkar, S Chavhan, N Kunda, I Saleem, S Somavarapu, KM Taylor, KK Sawant, Development of novel octanoyl chitosan nanoparticles for improved rifampicin pulmonary delivery: optimization by factorial design, AAPS Pharm. Sci. Tech. 19 (2018) 1758-1772. https://doi.org/10.1208/s12249-018-0972-9

75. G Ruiz-Pulido, D Quintanar-Guerrero, LE Serrano-Mora, DI Medina, Triborheological analysis of reconstituted gastrointestinal mucus/chitosan: TPP nanoparticles system to study mucoadhesion phenomenon under different pH conditions, Polymers. 14 (2022) 4978. https://doi.org/10.3390/polym14224978

76. JA Parish, JD Rivera, HT Boland, Understanding the ruminant animal digestive system, (2009). http://msucares.com/pubs/publications/p2503.pdf

77. R Qaqish, M Amiji, Synthesis of a fluorescent chitosan derivative and its application for the study of chitosan–mucin interactions, Carbohydr. Polym. 38 (1999) 99-107.https://doi.org/10.1016/S0144-8617(98)00109-X

78. S Chopra, S Mahdi, J Kaur, Z Iqbal, S Talegaonkar, FJ Ahmad, Advances and potential applications of chitosan derivatives as mucoadhesive biomaterials in modern drug delivery, Pharm. Pharmacol. 58 (2006) 1021-1032. https://doi.org/10.1211/jpp.58.8.0002

79. G Kali, P Knoll, A Bernkop-Schnürch, Emerging technologies to increase gastrointestinal transit times of drug delivery systems, J. Control Release. 346 (2022) 289-299.

80. H Katas, MA Raja, KL Lam, Development of chitosan nanoparticles as a stable drug delivery system for protein/siRNA, Int. J. Biomater. 2013 (2013) 146320. https://doi.org/10.1155/2013/146320

81. ML Tsai, RH Chen, SW Bai, WY Chen, The storage stability of chitosan/tripolyphosphate nanoparticles in a phosphate buffer, Carbohydr. Polym. 84 (2011) 756-761.

82. RC Nagarwal, PN Singh, S Kant, P Maiti, JK Pandit, Chitosan nanoparticles of 5-fluorouracil for ophthalmic delivery: characterization, in-vitro and in-vivo study, Chem. Pharm. Bull. 59 (2011) 272-278. https://doi.org/10.1248/cpb.59.272

83. HS Kim, SH Lee, CJ Eun, J Yoo, YS Seo, Dispersion of chitosan nanoparticles stable over a wide pH range by adsorption of polyglycerol monostearate, Nanomater. Nanotechnol. 10 (2020). https://doi.org/10.1177/18479804209172